Tectonophysics 770 (2019) 228222

Contents lists available at ScienceDirect

Tectonophysics

journal homepage: www.elsevier.com/locate/tecto

Comparing contiguous high- and low-elevation continental margins: New (U-Th)/He constraints from South Brazil and an integration of the thermochronological record of the southeastern passive margin of South America

Mathias Hueck[a,b,*], István Dunkl[a], Sebastián Oriolo[c], Klaus Wemmer[a], Miguel A.S. Basei[b], Siegfried Siegesmund[a]

[a] Geoscience Centre, Georg–August–Universität Göttingen, Göttingen, Germany
[b] Instituto de Geociências, Universidade de São Paulo, São Paulo, Brazil
[c] CONICET-Universidad de Buenos Aires, Instituto de Geociencias Básicas, Aplicadas y Ambientales de Buenos Aires (IGEBA), Argentina

A R T I C L E I N F O

Keywords:
Continental margins
(U-Th/He) thermochronology
Thermal modelling
Sul-rio-grandense shield

A B S T R A C T

The southeastern coast of South America is an example of the complexity of passive continental margins, as it displays both high- and low-elevation segments despite sharing a similar pre-rift geological history and structural configuration. As such, it is a prime candidate for investigating debated questions concerning the evolution of passive margins, such as the tectonic mechanisms driving uplift, their relationship to rifting and continental break-up, and why some margins are elevated when others are not. In this contribution, we present new (U-Th)/He data from a low-altitude portion of the South American passive margin in South Brazil, the Sul-rio-grandense Shield, and interpret it in the context of the regional thermochronological record. New results produce widespread apparent ages and reveal a complex exhumation history from the early Paleozoic onwards, including reheating during Paleo-Mesozoic sedimentation. For most of the study area, however, final exhumation was achieved at the latest during the rifting and early opening of the South Atlantic Ocean (135 Ma to 100 Ma). In spite of the presence of major Neoproterozoic shear zones, the inherited NE-SW structural framework seems not to have strongly influenced the thermochronological record. The new data were integrated into a large compilation of apatite fission track and (U-Th)/He results from southeast South America, in order to compare regional trends and investigate possible tectonic controls in the exhumation history. Low-elevation areas of the passive margin consistently record complex pre-rift cooling histories, while high-elevation areas experienced significant Upper Cretaceous/Paleogene uplift associated with the reactivation of Neoproterozoic shear zones. Because the inherited structural features of both segments are similar, plate dynamics alone cannot be responsible for the variating response. Hence, mantellic processes associated with post-rift alkaline magmatism may have affected the contrasting exhumation histories. This process was probably controlled by important South Atlantic fracture zones.

1. Introduction

Elevated passive margins occur in all continents and display varied geological characteristics, yet the tectonic mechanisms and processes behind their formation and maintenance remain controversial. The uplift of marginal plateaus has traditionally been interpreted as the result of rifting and/or continental break-up (e.g., Gilchrist and Summerfield, 1990; Chery et al., 1992). However, the preservation of uplifted rift flanks for more than tens of millions of years has been put in doubt (van der Beek et al., 1995), leading to variations in the mechanisms behind the preservation of high topographies (e.g. Sacek et al., 2012). A recurrent debate in recent decades has opposed such long-term evolutions with multi-event thermal histories that include one or more post-rift exhumation stages (Nielsen et al., 2009; Japsen et al., 2012; Green et al., 2018; Wildman et al., 2019 and references therein). Furthermore, many passive margins have low elevations, raising the question of why some margins are elevated while others are not.

* Corresponding author at: Instituto de Geociências, Universidade de São Paulo, São Paulo, Brazil.
E-mail address: mathiashueck@gmail.com (M. Hueck).

https://doi.org/10.1016/j.tecto.2019.228222
Received 6 May 2019; Received in revised form 16 August 2019; Accepted 6 October 2019
Available online 16 October 2019

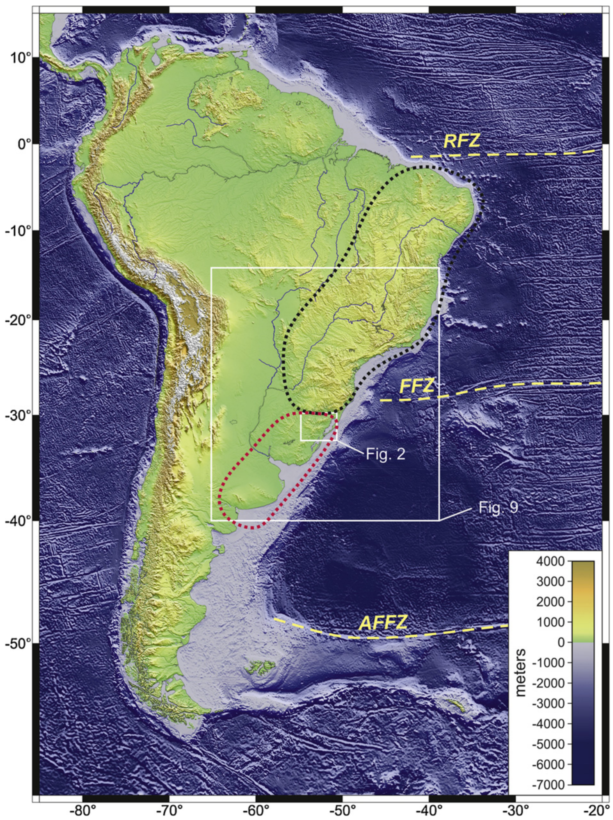

Fig. 1. Digital elevation model of South America and part of the South Atlantic Ocean. Elevated (black) and low-altitude (red) segments of the continental passive margin follow Green et al. (2018), and main fracture zones of the South Atlantic Ocean follow Torsvik et al. (2009). RFZ: Romanche Fracture Zone; FFZ: Florianópolis Fracture Zone; AFFZ: Agulhas-Falklands Fracture Zone. (For interpretation of the references to colour in this figure legend, the reader is referred to the web version of this article).

The South Atlantic coastline of South America is a classic example of an elevated passive margin, with the presence of a wide, elevated plateau in East Brazil with some altitudes of over 2500 m (Fig. 1). On the other hand, its southern segment between South Brazil and East Argentina is characterized by much gentler topographies and elevations characteristically below 500 m, commonly associated with the presence of gondwanic surfaces (Ab'Sáber, 2000; Demoulin et al., 2005; Panario et al., 2014). Nonetheless, the pre-rift structural configuration is similar for much of the extension of the margin, with large-scale Neoproterozoic lineaments parallel to the NE-SW direction of the continental margin itself (Basei et al., 2005, 2008; Heilbron et al., 2008; Passarelli et al., 2011; Egydio-Silva et al., 2018; Oriolo et al., 2018). Traditionally, most thermochronological research has concentrated in the km-high vertical profiles of the elevated ridges in East Brazil, recognizing extensive post-rift exhumation (Gallagher et al., 1994; Tello Saenz et al., 2003; Hackspacher et al., 2004, 2007; Hiruma et al., 2010; Cogné et al., 2011, 2012; Karl et al., 2013; Krob et al., 2019). More recently, however, investigations in the low-elevation sections of the continental margin have revealed a thermal history that extends well into the Paleozoic and has only limited evidence of post-rifting exhumation (Kollenz et al., 2016; Oliveira et al., 2016a; Hueck et al., 2017; Gomes and Almeida, 2019). In summary, these contrasting post-rift thermal histories between contiguous sectors of a passive margin with a similar pre-rift evolution mean that the region is ideal for investigating the mechanisms that can lead to the presence or absence of elevated margins.

In this paper, we discuss the exhumation history of the South American passive margin using new (U-Th)/He thermochronological data from a low-elevation region in South Brazil. After a brief introduction to the geological history of the study area we present the new data and use thermal modelling to discuss the complex exhumation history of the region. For this, we use a qualitative method for analyzing (U-Th)/He thermochronological data, considering frequent limitations of the method with over-dispersed results. After this, the discussion is expanded to the southern and central segments of the passive margin, with the presentation of a large compilation of apatite fission track and (U-Th)/He data collected between East Argentina and East Brazil. Along this study area, which shares similar pre-rift geological histories and structural configurations, we examine regional variations in the thermochronological record, the potential influence of Neoproterozoic shear zones in the exhumation history, and possible tectonic mechanisms behind contrasting patterns.

2. Geological context

2.1. Neoproterozoic framework

The South American Platform is a collage of Precambrian terranes amalgamated in the Neoproterozoic during the Brasiliano/Pan-African orogenic cycle, leading to the formation of West Gondwana (e.g., Almeida et al., 1981; Heilbron et al., 2008; Brito Neves and Fuck, 2014; Siegesmund et al., 2018). The eastern and southeastern portion of the platform, following the present-day South Atlantic shoreline, comprises the Mantiqueira Province, a composite of orogenic systems many thousands of km long. It is divided into three belts, from north to south: Araçuaí, Ribeira and Dom Feliciano. Throughout its extension, these belts share similar structural features, such as predominantly NE-SW large-scale lineaments, parallel to the South Atlantic coastline (Heilbron et al., 2008; Basei et al., 2010; Passarelli et al., 2011; Egydio-Silva et al., 2018; Oriolo et al., 2018).

The southernmost extent of the Mantiqueira Province in Brazil is the Sul-rio-grandense Shield, an exposition of Precambrian basement covering an area of ca. 50,000 km^2, bordered on all sides by Phanerozoic sediments (Fig. 2). The eastern portion of the shield includes the Dom Feliciano Belt, an orogenic system that extends from southern Brazil to Uruguay and is the result of the tectonic interaction between the Congo, Kalahari and Rio de la Plata cratons, along with smaller crustal fragments (Basei et al., 2000, 2005, 2008; Oyhantçabal et al., 2009; Oriolo et al., 2016a; Philipp et al., 2016; Hueck et al., 2018a). The belt is traditionally divided into three main units (Basei et al., 2000): an eastern (external) domain consisting of a granitic batholith; a central domain mainly comprising a metavolcano-sedimentary sequence in association with basement inliers; and a western (internal) domain, a foreland basin. These correspond, in the Sul-rio-grandense Shield, to the Pelotas Batholith, the Tijucas Terrane and the Camaquã Basin, respectively.

The first unit is a large association of granitic intrusions, recording the evolution from syn- to post-collisional stages between 650 Ma and 550 Ma, commonly associated with the activity of transcurrent shear zones (Silva et al., 1997; Philipp and Machado, 2005; Philipp et al., 2016). Occupying a central position in the Sul-rio-grandense Shield, the Tijucas Terrane is an association of Paleoproterozoic gneiss-migmatitic rocks (Hartmann and Chemale, 2003) and metavolcano-sedimentary sequences that record multiple metamorphic and deformation phases (Basei et al., 2008; Saalmann et al., 2011; Pertille et al., 2017). Deposited on top of the crystalline basement, the Camaquã Basin comprises five sedimentary cycles deposited between 600 Ma and 535 Ma, of which the last three were accompanied by intermittent volcanism (Wildner et al., 2002; Borba et al., 2006; Almeida et al., 2012; Janikian et al., 2012).

In addition, the Sul-rio-grandense Shield also includes two terranes that acted as foreland for the evolution of the Dom Feliciano Belt in the late Neoproterozoic. The São Gabriel Terrane is a Tonian-Cryogenian juvenile association, unique of its kind in the southern Mantiqueira

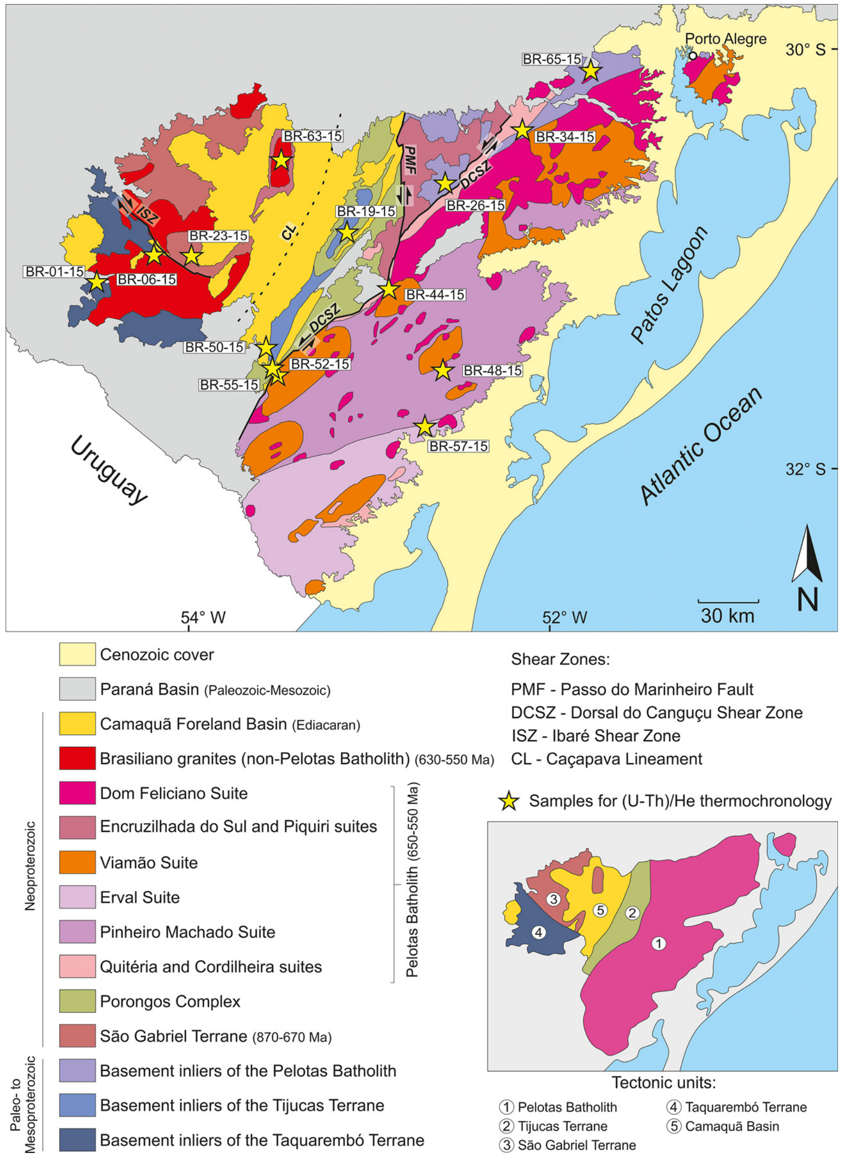

Fig. 2. Geological map of the Sul-rio-grandense Shield with location of the analyzed samples. The inset schematizes the main tectonic units. Modified from Wildner et al. (2006); Saalmann et al. (2011) and Philipp et al. (2016).

Province (Babinski et al., 1997; Hartmann et al., 2011; Lena et al., 2014; Philipp et al., 2018). It comprises two generations of magmatic arcs, along with numerous ophiolitic complexes and metamorphosed marginal deposits, intruded by granites during the evolution of the Dom Feliciano Belt. On the other hand, the Taquarembó Terrane is a Paleoproterozoic granulitic association intruded by Neoproterozoic granites during the Brasiliano/Pan-African orogenic cycle (Philipp et al., 2016). It represents a continuation of the Nico Pérez Terrane in Uruguay, which was accreted to the Rio de la Plata Craton in the Neoproterozoic (Oriolo et al., 2016b; Oyhantçabal et al., 2018).

All tectonic terranes are separated by major shear zones hundreds of km long, which define the main structural grain of the Sul-rio-grandense Shield (Fernandes et al., 1992; Philipp et al., 2016; Oriolo et al., 2018). The NW-SE-trending Ibaré Shear Zone separates the Taquarembó and São Gabriel terranes, while the latter is limited to the east by the NE-SW Caçapava Lineament, which separates it from the Tijucas Terrane. This structure is covered by the sediments of the Camaquã Basin and is predominantly recognized by geophysical methods. On its turn, the Tijucas Terrane is separated from the Pelotas batholith by the NE-SW-trending Dorsal do Canguçu Shear Zone, which is cut by the brittle Passo do Marinheiro Fault.

2.2. Post Brasiliano/Pan-African history

During the Paleo- and Mesozoic, large portions of the southern South American Platform were covered by the intracratonic Paraná Basin. During its sedimentary history, it experienced numerous cycles of subsidence and gaps in sedimentation, commonly associated with the far-field influence of orogenic processes in the southwestern margin of Gondwana (e.g., Zalán et al., 1990; Rocha-Campos et al., 2019). The onset of sedimentation was restricted to rift deposition in the Ordovician and Silurian, while the main sedimentary stage took place towards the end of the Paleozoic, with two supersequences deposited in large epicontinental seas connected to the ocean in the Devonian and Permian (Assine et al., 1994; Milani et al., 2007). The Mesozoic was characterized by the deposition of three more cycles in continental settings, with a restricted Triassic sedimentation and two regional cycles in the Cretaceous (Riccomini, 1997; Zerfass et al., 2004). Intermittent alkaline intrusions are found along the borders of the basin, beginning in the Permo-Triassic and spanning into the late Cretaceous (Almeida, 1991; Riccomini et al., 2005).

The most important magmatic event in the region, however, was the gigantic eruption of continental flood basalts in the early Cretaceous,

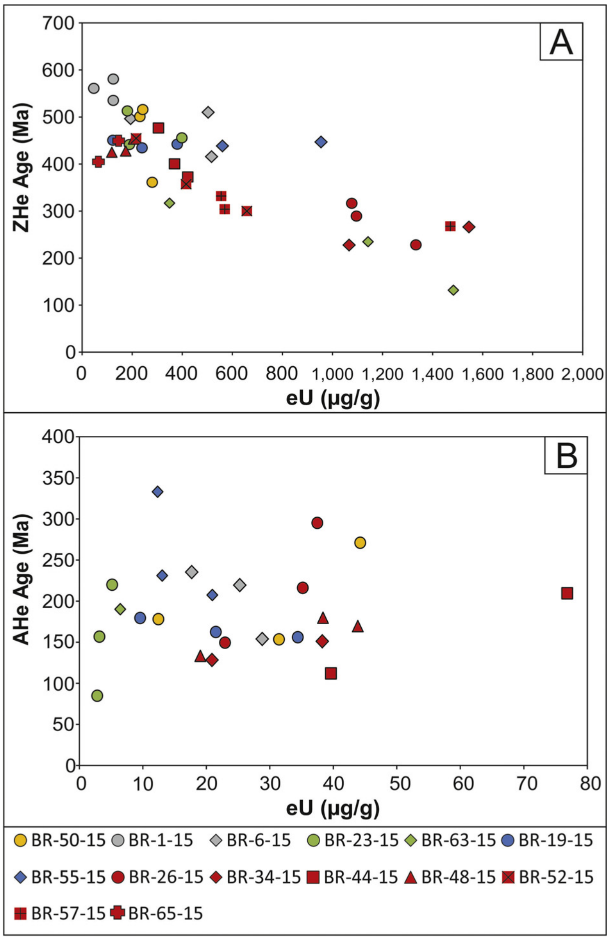

Fig. 3. Single-crystal zircon (a) and apatite (b) (U-Th)/He age versus eU content for the entire measured dataset, with the exclusion of obvious outliers, as discussed in the text. Symbols are color-coded according to the tectonic units of each of the samples: Orange – Camaquã Basin; Grey – Taquarembó Terrane; Green – São Gabriel Belt; Blue: Tijucas Terrane; Red: Pelotas Batholith. (For interpretation of the references to colour in this figure legend, the reader is referred to the web version of this article).

covering an area of over 1 million km^2 with up to 2 km of volcanic rocks. Remnants of this event are also found in Namibia and Angola. Most volcanic activity took place in a relatively short period, as available ages spread from 135 Ma to 131 Ma, but are mostly centered on 134 Ma (Renne et al., 1992; Thiede and Vasconcelos, 2010; Janasi et al., 2011; Pinto et al., 2011; Rossetti et al., 2018). This event, known as the Paraná-Etendeka Large Igneous Province (LIP), also includes intrusive units such as dyke swarms interpreted as feeding systems (Piccirillo et al., 1990; Florisbal et al., 2014) and large alkaline intrusions (Rossetti et al., 2018; Cañón-Tapia, 2018). The extrusion of the LIP was followed by the rifting and opening of the South Atlantic Ocean from the Hauterivian to the Albian, which progressed from south to north (Contreras et al., 2010; Moulin et al., 2010; Stica et al., 2014).

Intense exhumation affected the central segment of the South American passive margin following the continental break-up. This event culminated in the uplift of elevated ridges in Southeast Brazil with altitudes upwards of 2500 m. Major exhumation phases associated with the reactivation of large scale Neoproterozoic shear zones were recognized in these areas during the late Cretaceous-Paleocene and later in the Paleogene using thermochronological data (Tello Saenz et al., 2003; Hackspacher et al., 2004, 2007; Hiruma et al., 2010; Cogné et al., 2011, 2012; Karl et al., 2013; Krob et al., 2019). The southern portion of the continental margin, however, has a much lower topography, with elevations in the Sul-rio-grandense Shield mostly below 500 m. The thermal evolution suggested by previous thermochronological studies in the area is also in contrast with that of the elevated portion of the passive margin, as post-rift exhumation is much more restricted, limited to localized samples recording cooling in the order of a few tens of °C (Borba et al., 2002, 2003; Bicca et al., 2013; Kollenz et al., 2016; Oliveira et al., 2016a; Hueck et al., 2017; Gomes and Almeida, 2019).

3. (U-Th)/He thermochronology in the Sul-rio-grandense Shield

(U-Th)/He thermochronology was applied in the Sul-rio-grandense Shield for both zircon (ZHe) and apatite (AHe). These methods were chosen in order to complement the available thermochronological data in the study area, which is restricted to fission track analyses in zircon (ZFT) and apatite (AFT) (Borba et al., 2002, 2003; Bicca et al., 2013; Oliveira et al., 2016a; Gomes and Almeida, 2019). By integrating the new results with the available data (Section 3.3), the aim of this study is to recognize regional trends and test geological hypotheses for the thermal evolution of the study area (Sections 3.4 and 3.5).

34 individual samples were collected from the main crystalline basement units along three 100–200 km cross-sections oriented approximately E–W to NE-SW, covering all tectonic domains and cross-cutting all main shear zones. The low topographic prominence of the study area prevented the sampling along vertical profiles. Sampling was mostly focused on gneisses and granites but was not restricted to them. All samples were treated for mineral concentration using standard gravity and magnetic separation techniques. 14 samples were selected for (U-Th)/He dating based on the quality of the concentrated heavy minerals and on their location, aiming to cover the entire Sul-rio-grandense Shield and represent the main lithological units (the location of the samples is shown in Fig. 2, and the coordinates of the selected samples are presented in Appendix A). All of these samples yielded high-quality zircon and apatite, except for two samples (BR-57-15 and BR-65-15), which had only zircon. Individual crystals of each mineral were selected considering only euhedral, inclusion-free, clear crystals, preferentially with a minimum diameter of 60 µm and two intact terminations. We also performed an evaluation of radiation damage to zircon crystallinity with Raman spectroscopy prior to He measuring in order to exclude highly damaged crystals (e.g. Hueck et al., 2018b). Three single-crystal aliquots were selected for each sample, with the exception of samples BR-44-15 and BR-55-15, for which only two crystals of apatite and zircon, respectively, had acceptable quality. All analyses were performed at the GÖochron Laboratory of the University of Göttingen, following analytical procedures described in Appendix B. Results are presented in Appendix C.

3.1. Zircon

A total of 41 crystals were measured from 14 samples. All of them produced ZHe ages that are younger than the stratigraphic age of the sampled units, with the exception of a single crystal from sample BR-63-15, which was therefore discarded for the remaining analyses. The individual crystals yielded a wide spread of ages, between 580 Ma and 60 Ma. The results have no apparent correlation with such influencing factors as altitude or grain size, and the different ages are not arranged geographically into blocks with similar ages. There is, however, a moderate negative correlation between individual ages and the concentration of radioactive elements in the measured crystals (Fig. 3A), expressed in its effective uranium content (eU, U + 0.235 * Th, in µg/g). This negative correlation is a common feature of the (U-Th)/He thermochronological method for zircon, while apatite usually presents positive correlations. Both trends are caused by the fact that the accumulation of radiation damage in the crystalline structure of the measured crystals has an influence on its He retentivity (e.g., Flowers et al., 2009; Guenthner et al., 2013). Given enough time for the accumulation of radiation damage, it will effectively lead to distinct closure temperatures for individual crystals and, consequently, contrasting ages, even if they experienced the same thermal trajectory. Under appropriate conditions, this feature can be used for constraining detailed thermal histories by modelling an expected distribution of eU content vs. age and comparing it to the measured dataset (Ault et al., 2009; Flowers and Kelley, 2011; Guenthner et al., 2017; Johnson et al., 2017; Hueck et al., 2018b). In the new dataset, however, this correlation is quite broad along a wide extension of eU contents (0 μg/g to 1600 μg/g), varying from apparent ages of ca. 500 Ma to ca. 200 Ma, and with variations of up to 100 Ma for a given eU value. As such, it does not correspond to a single thermal history shared by all analyzed samples, preventing its use as a modelling tool using the current diffusion models (Guenthner et al., 2013).

Nonetheless, this correlation can be used as a criterion for identifying the most representative ages within the dataset. Based on the eU content of all measured zircon crystals, the dataset can roughly be divided into two groups. The first one comprises the majority of crystals (30) and is characterized by eU values up to 700 μg/g and ZHe ages between 580 Ma and 300 Ma. On the other hand, the second group corresponds to 10 crystals with eU values between 950 μg/g and 1600 μg/g, which produced consistently younger apparent ages, almost all of them below 300 Ma. These ages are already well in the range of the AHe dataset and published AFT results for the same region (mostly 330 Ma to 100 Ma, Borba et al., 2002, 2003; Bicca et al., 2013; Oliveira et al., 2016a; Gomes and Almeida, 2019), which will be discussed in more detail in the next sections. The excessively young ages suggest that the He retentivity of these crystals is significantly poorer than what is commonly assumed for the ZHe system, effectively shifting their partial retention zone (PRZ) to temperatures comparable to those of apatite thermochronometry. Although this cannot be successfully modelled, enhanced He diffusion was probably caused by the accumulation of radiation damage in the measured crystals' lattice, expressed in the elevated eU values. This is supported by the fact that there is a moderate correlation in our dataset between the eU content of individual zircon crystals and the width of the $\nu 3$ (SiO_4) Raman band at ~1000 cm^{-1} (Fig. 4), which is a proxy for estimating alpha-radiation damage (Nasdala et al., 2001; Palenik et al., 2003; Hueck et al., 2018b). For these reasons, only the first group is assumed to have ages representative of the traditional temperatures for the ZHe PRZ, a distinction that will be acknowledged in subsequent discussions of the dataset. It should be noted that a similar pattern was observed in the northern part of the Dom Feliciano Belt, where the ZHe ages from crystals with eU contents above 1000 μg/g consistently yielded ages comparable to AHe results in the same samples (Hueck et al., 2018b).

3.2. Apatite

In total, 35 apatite crystals from 12 samples were analyzed, resulting in a wide array of apparent AHe ages. A few of the results are

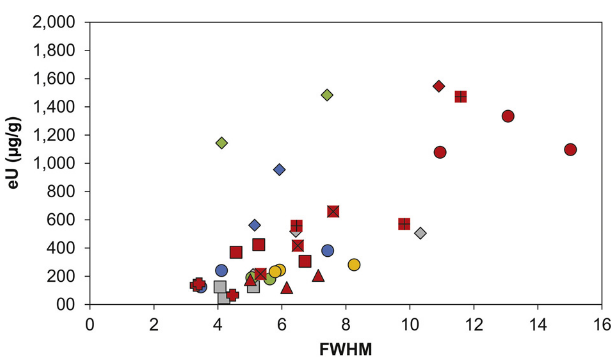

Fig. 4. Full width at half measure (FWHM) of the $\nu 3$ (SiO_4) Raman band at ~1000 cm^{-1} of measured zircons *versus* eU content for all measured zircons. Symbol legend and color-coding is the same as in Fig. 3.

considered outliers. These correspond mostly to individual crystals which are much older than the vast majority of ages, including a few that are older than the stratigraphic age (as in sample BR-52-15) or older than the corresponding ZHe age measured in the same sample (BR-63-15). These crystals have grain sizes and eU contents that are similar to those of the rest of the dataset, and may have been influenced by small inclusions that could not be identified. A different case of outlying ages is that of crystals from sample BR-1-15, which yielded ages much younger than those of the remaining dataset. These crystals are also characterized by extremely low U and Th contents and, as a consequence, produced very little He during extraction of the gas, which might have influenced the results. Although very low eU contents have the effect of causing younger apparent ages due to enhanced He diffusion, (e.g., Ault et al., 2009; Flowers et al., 2009; McDannell et al., 2018), the outlying ages are far younger than what could be attributed to this effect.

Excluding the outlying crystals discussed above, the measured AHe ages do not correlate with possible influencing factors such as altitude, grain size or eU content (Fig. 3B), and are not distributed according to geographical location. Notwithstanding, they cover a wide range of possible apparent ages between 333 Ma and 85 Ma, with a majority of results concentrated between 235 Ma and 100 Ma. Within this time interval, the individual ages show a continuous distribution, without the presence of apparent age gaps or concentration into particular periods. The lack of an individual controlling factor that might explain the distribution of the AHe dataset suggests that they cannot be resolved with a single thermal history, and that the analyzed samples probably underwent at least slightly different T-t trajectories. Furthermore, the continuous spread of ages throughout a long period of time also indicates a prolonged permanence under temperature conditions at or close to the PRZ of the system, without fast heating or cooling events.

3.3. Integrating the new dataset with published thermochronological data

The new (U-Th)/He results add to previously published thermochronological data of the Sul-rio-grandense Shield (Fig. 5), though the conciliation between the different applied methods is not always straightforward. In particular, there is a clear contradiction between the new ZHe ages and the only previously reported ZFT ages from the study area (Oliveira et al., 2016a). Although the latter ages correspond to a thermochronometer with a higher annealing temperature, the reported ages are distributed between 386 Ma and 210 Ma, which are predominantly younger than the low-eU ZHe ages presented in this study (Section 3.1). Furthermore, most ZFT apparent ages are comparable with the oldest AFT and AHe ages in the region. This contradiction may be in part caused by contrasting sampling strategies, as all ZFT measurements were obtained from samples of sedimentary rocks of the Camaquã Basin, while the new (U-Th)/He ages represent a variety of units from the crystalline units the Sul-rio-grandense Shield. This distinction alone should not explain the inconsistent ages, as the sediments from the Camaquã Basin overly the basement units and should therefore have apparent ZFT ages at least as old as the suggested ZHe interval. However, the application of different methods for different kinds of rocks may have ultimately influenced the results, considering that zircons from sedimentary rocks typically have a much wider compositional spread of detrital grains than that of monogenetic basement units, implicitly affecting crystal selection during analytical procedures. In addition, the application of fission-track thermochronometry in high-U zircons with long expositions beneath the partial annealing zone offers particular challenges, as these crystals commonly present uncountable track densities which can lead to biased results (e.g. Malusà et al., 2013 and references therein). In fact, this is one of the reasons why we opted to apply the (U-Th)/He method for zircon in the study area. Alternatively, the apparently contradicting results could represent contrasting thermal regimes between the Camaquã Basin and its crystalline basement. In any case, the relative consistency of the new ZHe

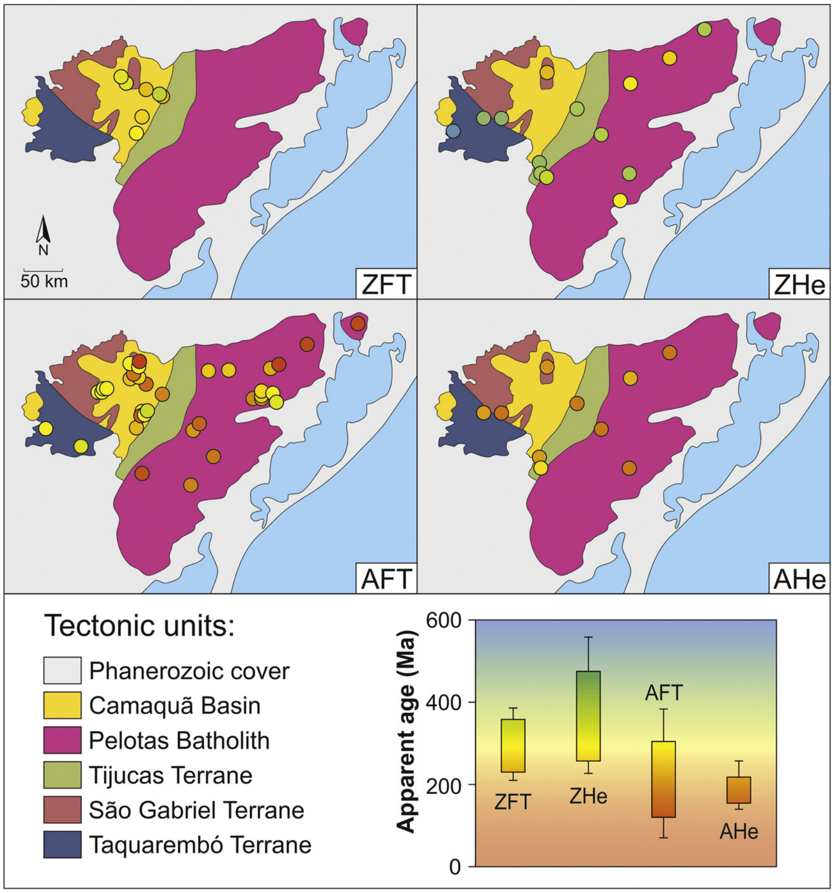

Fig. 5. Comparison of the results for zircon and apatite fission track (ZFT and AFT) and (U-Th)/He (ZHe and AHe) thermochronometry in the Sul-rio-grandense Shield, with data from Borba et al., 2002, 2003, Bicca et al., 2013; Oliveira et al., 2016a; Gomes and Almeida, 2019 and this study. Each sample is represented by its apparent age, following the same color palette as in the inset diagram in the lower right corner. The maps represent all samples collected in the surface or in the shallowest levels of a drill core. Whenever a given sample has more than one fission track age in the literature, only one age is represented, unless the difference is very significant. The ZHe dataset includes samples which only yielded high-eU crystals in order to represent the entire range of samples and results (see section 3.1 for more details). The inset diagram represents the entire range of apparent ages for all methods in the study area, with 75% of the results contained in the boxes.

dataset throughout a larger sampling area and the use of the eU content as an internal control of the ZHe apparent ages allow us to consider these ages representative of cooling below 140 °C to 180 °C for the crystalline basement. A similar and even older range of ZHe ages (550 Ma to 450 Ma) from the analogous Precambrian Shield of Uruguay further supports the consistency of the new dataset (Hueck et al., 2017).

On the other hand, in the lowermost temperature range, the interval of new apparent AHe ages is very similar to that of previous thermochronological studies performed in the Sul-rio-grandense Shield. AFT ages reported in the study area span a wide range between 385 Ma and 70 Ma (Borba et al., 2002, 2003; Bicca et al., 2013; Oliveira et al., 2016a; Gomes and Almeida, 2019), with most ages concentrated between 305 Ma and 120 Ma. Taken together, while the results for both the AFT and AHe are remarkably dispersed, they describe a consistent general trend. As such, the large spread in apparent ages cannot be ascribed solely to the inherent dispersion of each method in the context of a unifying exhumation history. Instead, it indicates a complex evolution for the study area, on which different samples likely experienced contrasting thermal trajectories, as also suggested by Oliveira et al. (2016a), which modelled numerous distinct T-t paths throughout the shield.

3.4. Thermal modelling

The application of thermal modelling for the new (U-Th)/He dataset should be approached with caution. In spite of the use of eU as a proxy for closure temperatures, the current models for the estimation of He diffusion and retention still suggest some inconsistencies for both zircon and apatite (e.g., Johnson et al., 2017; Green and Duddy, 2018; Hueck et al., 2018b). Non-quantifiable factors can also influence the apparent ages, including micro-inclusions, internal zonation, He trapping in microvoids, He implantation from neighboring radioactive phases and Cl content in apatite (Spiegel et al., 2009; Flowers and Kelley, 2011; Ault and Flowers, 2012; Gautheron et al., 2013; Orme et al., 2015; Zeitler et al., 2017; McDannell et al., 2018). All of these can lead to a frequent over-dispersion of the results (Green and Duddy, 2018). In addition, as discussed in the previous sections, different samples from the studied area probably underwent slightly different T-t trajectories. Taken together, these problems may ultimately compromise the possibility of performing He-based thermal modelling in order to constrain detailed T-t trajectories. Therefore, the aim of this section is not to obtain precise thermal histories, but rather to provide a qualitative comparison of possible geological scenarios, considering well-known geological constraints. In particular, thermal modelling was applied in order to evaluate whether (U-Th)/He results can best be described by a simple long-lasting exhumation history or by multiple stages of heating and cooling.

For this, we used the HeFTy program (Ketcham, 2005) and followed the zircon diffusion model of Guenthner et al. (2013) and apatite diffusion model of Flowers et al. (2009). In spite of the aforementioned limitations of these models, they are still the best approximation of the behavior of He diffusion currently in use. Individual crystal ages were corrected for alpha ejection according to Ketcham et al. (2011). For each modelled scenario, random T-t paths were tested within the boundaries of assumed constraints, yielding crystal diffusion curves that were on their turn compared with the ones calculated from the input data. According to their goodness of fit, satisfactory results were categorized into acceptable and good paths, considering minimum statistic values of 0.05 and 0.5, respectively (see Ketcham, 2005 for more details). All samples from the crystalline basement of the Sul-rio-grandense Shield that provided both acceptable ZHe and AHe ages were modelled, totalizing seven samples. Models were tested considering all measured zircon and apatite crystals for a given sample, but in a few samples the number of modelled crystals had to be reduced from three

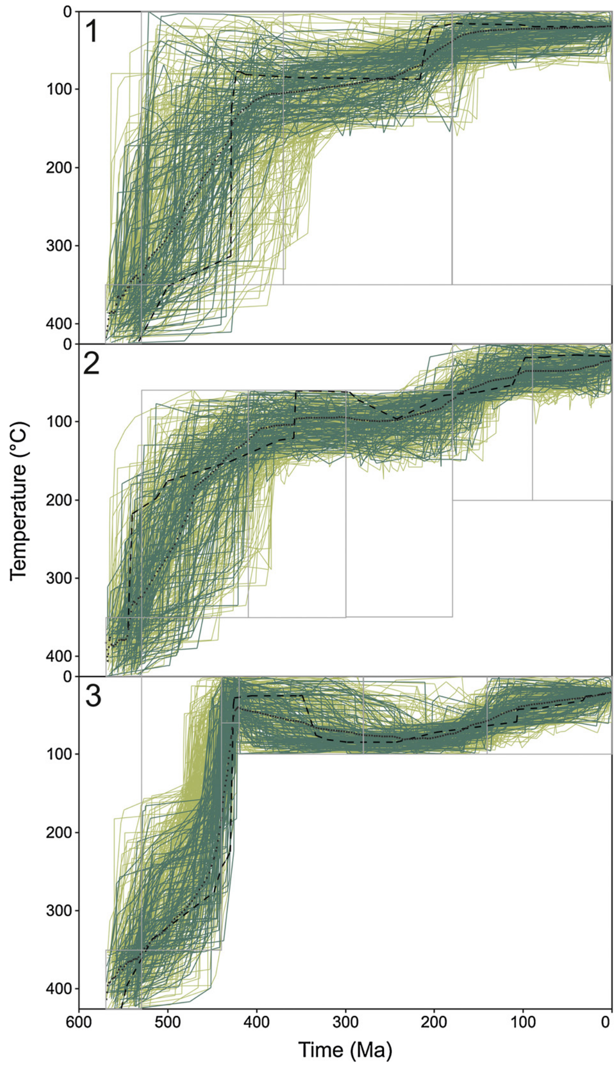

Fig. 6. Example of the thermal modelling applied to the (U-Th)/He dataset, with results from sample BR-55-15. The model tested in scenario 1 corresponds to an unsupervised model, on which only initial and final constraints are fixed. Scenarios 2 and 3 test two different geological hypotheses, simulating a thermal evolution with no exposition to near-surface conditions (T < 60 °C) prior to the mean AHe age of the sample, and an exposition to near-surface conditions in the Silurian, respectively. Note that both scenarios 2 and 3 were successfully predicted by the unsupervised model. Light and dark green paths correspond to acceptable and good paths, respectively, dashed and pointed lines represent best and mean paths, respectively, and grey boxes indicate the thermal constraint assumed for the simulations. (For interpretation of the references to colour in this figure legend, the reader is referred to the web version of this article).

to two for mineral phase due to bad performances of the Hefty program. As discussed above, zircons with eU content above 1000 μg/g were not considered for this thermal modelling, as they seem not to be representative of the PRZ temperatures considered for ZHe in the model by Guenthner et al. (2013). Additional details on the setup of the tested models are presented in Appendix B, while the values of all assumed constraints and a summary of the obtained results are presented in Appendix D. Appendix E presents the modelled thermal histories for all tested samples.

Initially, all samples were submitted to an unsupervised model (Scenario 1, Fig. 6), for which only initial and final conditions were fixed. Initial conditions were constrained at temperature ranges corresponding to the cooling of the muscovite K-Ar system (ca. 350 °C–425 °C, Purdy and Jäger, 1976; Harrison et al., 2009), in the Sul-rio-grandense Shield, set between 570 Ma and 530 Ma (Philipp et al., 2003, 2016). The present-day annual surface temperature, on the other hand, was set to 20 ± 5 °C. The main objective of these unsupervised models is to provide a base for comparison with the following modelling steps, which will test possible geological constraints. By comparing these initial results with the later ones, it will be possible to evaluate if the imposition of additional constraints increase or decrease the success rate of modelling a given dataset.

Following this step, two main viable thermal trajectories were tested for each of the basement samples, based on the geological evidence for the sedimentary history of the Sul-rio-grandense Shield. Both scenarios correspond to T-t paths that are in accordance with the range of possibilities obtained in the unsupervised models. The first one (Scenario 2, Fig. 6) assumes that the crystalline basement went through long-term cooling since the end of the Brasiliano/Pan-African orogenic cycle, and did not experience previous exposure to near-surface conditions. For this scenario, the only additional constraint was that the model was not allowed to explore paths with temperatures below 60 °C until the mean AHe age of each sample. The second hypothesis (Scenario 3, Fig. 6) assumes an initial exhumation to near-surface conditions during the early Paleozoic, after the thermal relaxation following the Brasiliano/Pan-African orogenic cycle and the formation of the Dom Feliciano Belt. This hypothesis allows the basement to be exposed prior to the onset of regional subsidence in the Paraná Basin, starting in the Devonian (Milani et al., 2007). It was constrained by fixing temperatures below 60 °C in the Silurian, between 440 Ma and 420 Ma. After this, the model was allowed to test for reheating, in order to simulate the deposition of the Paraná Basin. Temperatures from the Devonian onwards were limited at 100 °C. This value is a maximum estimation using maturation studies from sediments within the basin (Silva and Cornford, 1985) and assuming higher temperatures for the buried basement. The constraints imposed by this latter scenario are in agreement with the majority of the representative low-eU ZHe ages, which are predominantly older than 420 Ma.

The only sample that was not tested for scenarios 2 and 3 was Sample BR-50-15, which corresponds to a conglomerate from the Camaquã Basin, and therefore underwent a different thermal history than that assumed for the crystalline basement. For this sample, we performed an unsupervised modelling considering as an initial constraint surface conditions during deposition time, and limited the maximum temperatures to 100 °C, similar to the conditions tested in Scenario 3. The aim of this model was to test if our data could be reproduced with thermal trajectories compatible with the two tested hypothesis for the remaining samples. Finally, it should be noted that the impact of considerable thermal influence from the Lower Cretaceous volcanism of the Paraná-Etendeka LIP was not tested during thermal modelling, as an overwhelming majority of AHe ages are older than 135 Ma, thus indicating that this thermochronometer was already closed at the onset of magmatism and remained so afterwards.

Each simulation was tested for a total of 100,000 trajectories, or until 100 good fits were identified. The thermal modelling yielded quite successful results for the (U-Th)/He dataset, with most scenarios identifying numerous acceptable and good paths, commonly reaching 100 good paths before testing 100,000 possible trajectories. On a first order, this indicates that both tested hypotheses represent viable geological histories for the measured (U-Th)/He dataset.

There is, however, a noticeable difference between the success rates of the different tested scenarios in the samples that could be tested for both. When comparing the number of good paths in relation to the total paths tried for each simulation of a given sample, the second hypothesis (Scenario 3) consistently outperforms both the first Hypothesis (Scenario 2) and the unsupervised models (Scenario 1), suggesting a better compatibility with the modelled dataset (Fig. 7). In addition, in most cases, the first hypothesis (Scenario 2) yielded a performance considerably below that of the unsupervised models (Scenario 1), which means that the imposition of the tested T-t constraints resulted in less

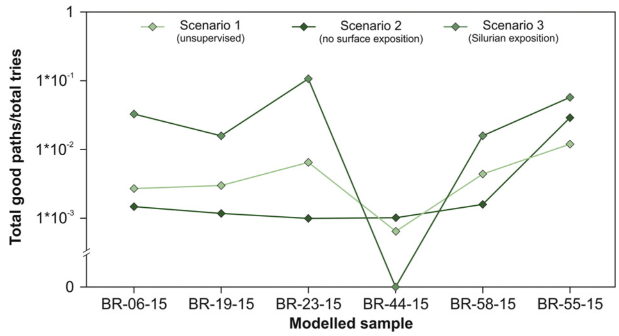

Fig. 7. Comparison of the performance of scenarios 1, 2 and 3 (as exemplified in Fig. 6) for all samples in which they could be tested. The Y axis represents the ratio of good fits in relation to the total number of tested paths for each simulation, in logarithmic scale (with the representation of zeroed ratios in models for which no good fits were found). All models were run 100,000 times or until obtaining the 100th good fit.

successful simulations than those with no constraints at all. The only exception to this pattern is that of Sample BR-44-15, for which no good-fitting thermal paths were identified for Scenario 3. Nonetheless, considering the majority of tested models, the results indicate that the assumption of an exposition to near-surface conditions prior to the sedimentation of the Paraná Basin, followed by reheating of the basement units due to basin subsidence is a more realistic depiction of the thermal evolution of the Sul-rio-grandense Shield. This is in agreement with results of the unconstrained model for sample BR-50-15, from the Camaquã Basin, for which the best matching thermal trajectories indicate a long period of heating up to ca. 80–100 °C in the Paleo-Mesozoic (Appendix E).

3.5. Implications for the post-Brasiliano/Pan-African evolution of the Sul-rio-grandense Shield

The wide range of apparent ages in the new (U-Th)/He dataset hinders straightforward interpretations and should be interpreted with caution. The moderate correlation observed between ZHe ages and eU contents in the new results is probably a result of accumulated radiation damage in the measured crystals, leading to effectively variable closure temperatures (Guenthner et al., 2013, 2017; Johnson et al., 2017). While this broad correlation cannot be interpreted in terms of a single unifying coherent thermal history, single-crystal eU content can be used as an internal criterion for selecting the most representative analyses. Those are consistently older than 300 Ma, and are mostly grouped between 550 Ma and 400 Ma. This indicates that considerable exhumation in the early Paleozoic followed the late stages of the Brasiliano/Pan-African orogenic cycle (ca. 550 Ma, Philipp et al., 2016; Hueck et al., 2018a, c). The lack of a unified thermal history for the shield in this period indicates local variations in the thermal history during exhumation through the ZHe PRZ, which might be a consequence of fault-bounded block tectonics. This is supported by unpublished K-Ar ages of illite from fault gouges collected throughout the shield (Hueck et al., manuscript in preparation), indicating recurrent fault activity in the early Paleozoic. The influence of fault activity and block segmentation was also recognized during the Paleozoic sedimentation of the Paraná Basin (e.g., Holz et al., 2006).

The new thermal modelling results support the possibility of an Early Paleozoic exhumation for most of the shied. Comparative analyses between different thermal histories suggest that most of the shield was probably exposed to near-surface conditions in the early Paleozoic and then reheated during the deposition of the Paraná Basin. This is in accordance with the sedimentary contact between the crystalline basement and Devonian units in the eastern border of the shield (Fig. 2). Similar T-t trajectories characterized by initial exhumation to near-surface conditions followed by reheating during the Paleozoic were recognized for other expositions of crystalline basement rocks along the Dom Feliciano Belt, as in the case of the basement shields in Uruguay and Santa Catarina (Hueck et al., 2017, 2018b; Krob et al., 2019). These observations reinforce the idea that the South American platform experienced quite eventful cycles of burial and exhumation during the Paleo-Mesozoic, in spite of its position in the interior of Gondwana. This is in accordance with the interpretation that the sedimentary evolution of the continental basins in the region have been controlled by the far-flung tectonic influence of orogenic pulses in the active margin of the supercontinent (Zalán et al., 1990; López-Gamundi and Rosello, 1993; Zerfass et al., 2004; Milani et al., 2007; Rocha-Campos et al., 2019).

Similarly to the ZHe data, the new AHe results are widespread, with single-crystal apparent ages between 333 Ma and 85 Ma, but mostly concentrated between 235 Ma and 100 Ma. Individual crystal ages are dispersed continually in this age range, suggesting that they experienced no rapid cooling. Instead, a long-term residence in the PRZ was probably promoted by the thermal effect of the Paraná Basin sedimentation, and final exhumation was only obtained after its erosion. As in the case of the ZHe system, the AHe age distribution cannot be modelled into a single thermal history, indicating that the different analyzed samples probably experienced slightly different T-t evolutions.

The most intuitive explanation for these distinct thermal histories is the reactivation of major structures inherited from its Neoproterozoic amalgamation (e.g., Gomes and Almeida, 2019). However, the compilation of new and available AFT and AHe data suggests that this interpretation is not straightforward (Fig. 8). The different terranes of the Sul-rio-grandense Shield fall into two main ranges of apparent ages. The first one includes the Camaquã Basin and the Taquarembó Terrane, and is mostly restricted between 400 Ma and 250 Ma, while the second group concentrates ages between 300 Ma and 100 Ma in the Pelotas Batholith and in the São Gabriel and Tijucas terranes.

In the latter case, the three terranes produced quite similar ranges of apparent ages, despite being separated by the two main NE-SW structures of the Sul-rio-grandense Shield, the Caçapava Lineament and the

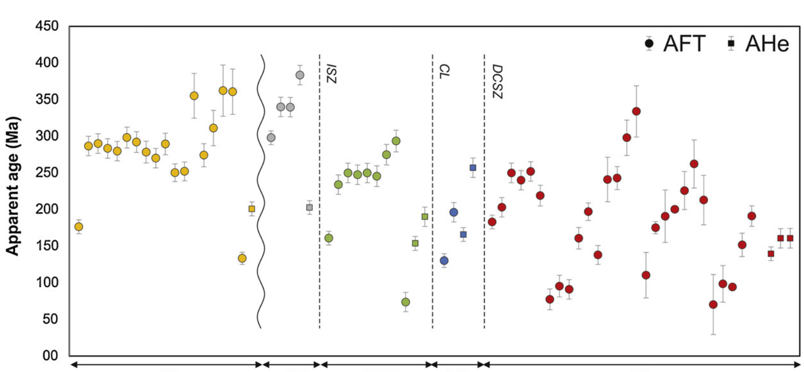

Fig. 8. Compilation of apatite fission track (AFT) and (U-Th)/He (AHe) thermochronological data for the Sul-rio-grandense Shield, with data from Borba et al., 2002, 2003, Bicca et al., 2013; Oliveira et al., 2016a; Gomes and Almeida, 2019, and this study. Results are organized according to the terrane of the corresponding samples, and the main structural features of the studied area are represented schematically. CB – Camaquã Basin; TT – Taquarembó Terrane; SGT – São Gabriel Terrane; TjT – Tijucas Terrane; PB – Pelotas Batholith; ISZ – Ibaré Shear Zone; CL – Caçapava Lineament; DCSZ – Dorsal do Canguçu Shear Zone. The wavy line between CB and TT represents a cover/basement relationship that extends to the whole shield.

Dorsal do Canguçu Shear Zone. This suggests that these structures apparently exerted little influence in the apatite thermochronological record of the bordering terranes, with intra-block age spreads in the same range as inter-block variations. This is somewhat surprising, as these two structures represent some of the most significant tectonic features of the shield. The Dorsal do Canguçu Shear Zone, in particular, is interpreted as part of a lineament following the entire length of the Dom Feliciano Belt for over 1000 km (Basei et al., 2000, 2018; Passarelli et al., 2011; Oriolo et al., 2018; Hueck et al., 2018a, c).

On the other hand, the Camaquã Basin and the Taquarembó Terrane yielded consistently older ages than the rest of the shield. In the case of the basin, this contrast may suggest a thermal evolution somewhat different from that of the rest of the Sul-rio-grandense Shield, as also suggested by the contradicting ZFT and ZHe results (Section 3.3). The case of the relatively old apparent ages from the Taquarembó Terrane, however, may in fact be an impact of recent reactivations of the Ibaré Shear Zone, which separates it from the bordering São Gabriel Terrane. This shear zone stands out for being the only one among the main Neoproterozoic lineaments of the shield to have a NW-SE direction.

The new AHe ages are in agreement with previous AFT results, and are virtually exclusively older than ca. 100 Ma (Section 3.3). This suggests that, for most of the Sul-rio-grandense Shield, final exhumation to near-surface conditions was acquired at the latest by the time of rifting and break-up between Africa and South America (135 Ma to 100 Ma, Contreras et al., 2010; Moulin et al., 2010; Stica et al., 2014). Indeed, the new thermal models agree with previous results in the area, indicating that post-rift cooling is restricted to a few samples and did not involve more than a few tens of °C (Oliveira et al., 2016a; Gomes and Almeida, 2019; Appendix E). In addition, the extrusion of the voluminous Paraná-Etendeka LIP did not cause resetting of the AHe system, suggesting that, if the studied area was ever covered by flood basalts, they were not as thick as in the central portions of the basin (e.g. Hueck et al., 2018b).

4. Comparing the evolution of the high- and low-elevation sectors of the passive margin of South America

4.1. Thermochronological data in the southern and central passive margin of South America

The new (U-Th)/He results reveal that the Sul-rio-grandense Shield experienced a multi-phase thermal history during the Paleo- and Mesozoic with limited post-rift exhumation. In order to compare this evolution along a wider extension of the continental margin, thermochronological data (both AHe and AFT) from the southern to southeastern portion of the South American passive margin were compiled along the extension of the Mantiqueira Province (Fig. 9). We chose this tectonic entity as the main criterion for the delimitation of the area because, throughout its extension, it displays a similar structural configuration characterized by predominantly coast-parallel NE-SW structures inherited from the Neoproterozoic Brasiliano/Pan-African orogenic cycle (Basei et al., 2005, 2008; Heilbron et al., 2008; Passarelli et al., 2011; Egydio-Silva et al., 2018; Oriolo et al., 2018). Along almost 3000 km of extension, the main structural features of this orogenic association have only slight changes in obliquity from NE-SW in the south to ENE-SWS in the central portion, with overall variations in the order of 10° to 20° (Fig. 9A). Nonetheless, in spite of its shared structural framework, both elevated plateaus and low-elevation segments occur along its length (Fig. 9B and C). Because of these contrasting patterns between areas with similar pre-rift configurations, this area is of particular interest for investigating processes behind the exhumation and uplift of continental passive margins (e.g. Green et al., 2018; Wildman et al., 2019 and references therein). The aim of this compilation, therefore, is to evaluate the impact of the inherited Neoproterozoic structural framework and to discuss possible mechanisms in the exhumation history of the area.

The compilation follows a similar review by Oliveira and Jelinek, 2017, with the addition of AHe data and more recent AFT results, and comprises data from Gallagher et al. (1994); Oliveira et al. (2000, 2016a, 2016b), Borba et al. (2002, 2003), Jelinek et al. (2003, 2014), Tello Saenz et al. (2003); Hackspacher et al. (2004, 2007), Franco et al. (2005); Ribeiro et al. (2005); Franco-Magalhães et al. (2010, 2014), Hiruma et al. (2010); Cogné et al. (2011, 2012), Bicca et al. (2013); Karl et al. (2013); Souza et al. (2014); Kollenz (2015); Kollenz et al. (2016); Hueck et al., 2017, 2018b, Gomes and Almeida (2019) and Krob et al. (2019).

Throughout the extension of the Mantiqueira Province, young AFT and AHe apparent ages are predominantly concentrated in eastern and southeastern Brazil, which comprise elevated ridges (Figs. 9D, 9E, 9 F). Most results in these areas are Upper Cretaceous to Paleogene in age, predominantly younger than 100 Ma, and are therefore younger than the rift stage of the South Atlantic Ocean, which is constrained from the Hauterivian to the Albian (Contreras et al., 2010; Moulin et al., 2010; Stica et al., 2014).

On the other hand, this signature is markedly different from the thermochronological record from the low-elevation segments of the coastline in its southern extent. In these regions, as exemplified in the new dataset from the Sul-rio-grandense Shield, partial ages span hundreds of millions of years, and may extend to ages close to 400 Ma. This reveals not only a more complex thermal evolution, but also an exhumation history mostly restricted to the pre- to syn-rift stages of the South Atlantic Ocean. Even the most recent results in these regions are rarely younger than 135 Ma to 100 Ma, and thermal models only recognize localized and limited post-rift cooling. Therefore, it can be interpreted that, in contrast with the elevated portions, the low-elevation segments of the South American passive margin had mostly achieved final exhumation by the time of continental break-up.

Nonetheless, there is no direct correlation between sample elevation and apparent AFT and AHe ages, with a comparison yielding a rather broad pattern in which no discernible trends are recognized (Fig. 10). This suggests that, in spite of the general coincidence between young apparent ages in segments of the passive margin that have high-elevation areas and older ages in segments characterized by lower elevations, there is no homogeneous altitude control along the Mantiqueira Province, as should be expected for such a large study area.

4.2. Possible tectonic mechanisms

The elevated segments of the South American passive margin are usually interpreted as the result of post-rifting uplift (Hiruma et al., 2010; Cogné et al., 2011, 2012; Karl et al., 2013; Krob et al., 2019). The compilation presented here reinforce this interpretation, as it evidences that high-altitude plateaus coincide with areas in which AFT and AHe ages are predominantly Upper Cretaceous to Paleogene. This well constrained thermochronological history is not necessarily characteristic of elevated continental margins throughout the world. There is no similar consensus, for example, on the evolution of the elevated passive margins in the North Atlantic in Scandinavia and Greenland. Less constrained thermochronological data in these areas can alternatively be interpreted as evidence for or against a post-rift history of uplift (Nielsen et al., 2009; Japsen et al., 2012; Green et al., 2018; Wildman et al., 2019 and references therein).

On the other hand, the new data presented in Section 3 and the compilation of thermochronological data highlight how the thermal evolution of the South American passive margin is not homogeneous, as low-elevation portions did not experience such extensive post-rift uplift (Fig. 11). Hence, it is worth discussing the main mechanisms that have been proposed for the formation of the elevated margin in Eastern Brazil, discussing how they are in agreement or disagreement with the evolution of the low-altitude portions of the continental margin.

Two main causes have commonly been postulated for the extensive uplift in SE and central Brazil. The first one suggests that phases of

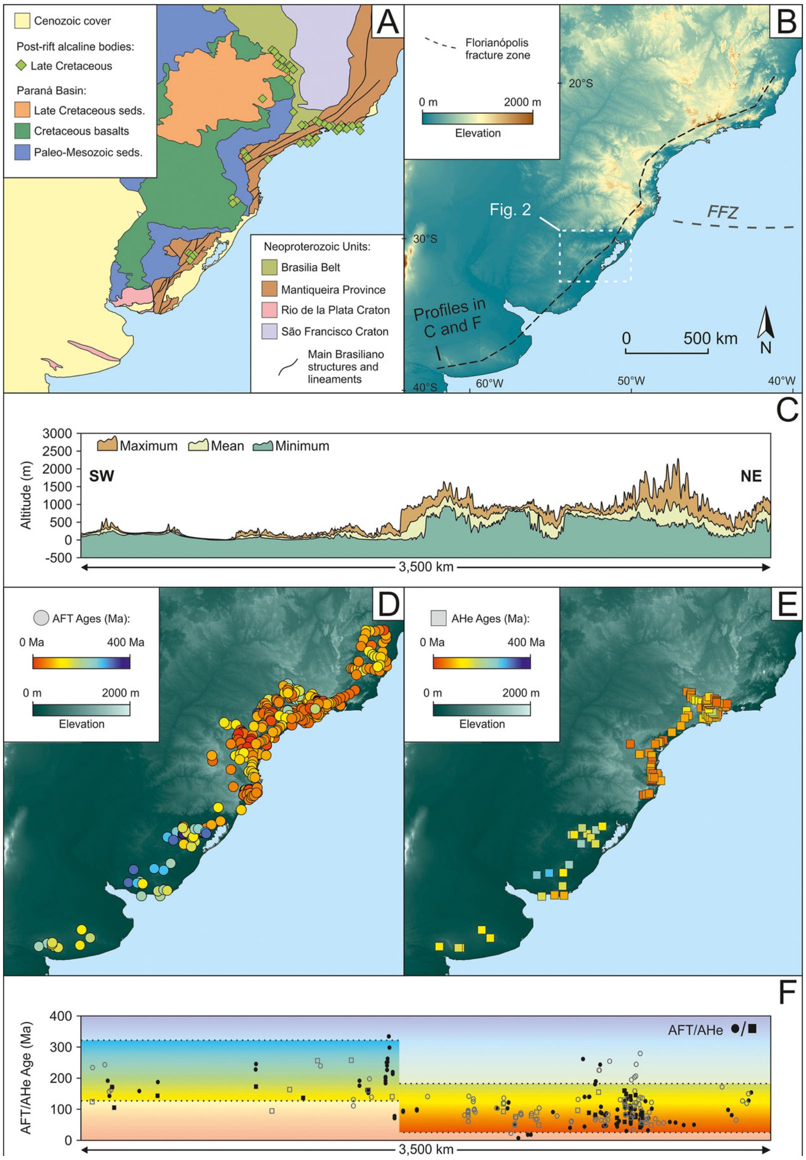

Fig. 9. Compilation of apatite thermochronological data and geological features related to post-rift exhumation in the southern and southeastern portions of the South American passive margin. A: Simplified geological map of the area, with Precambrian domains of the South American Platform, main structural features of the Mantiqueira Province and units of the Paraná Basin, and location of the main post-rift alkaline bodies along the passive margin. After Assine et al. (1994); Heilbron et al. (2008); Riccomini et al. (2005); Passarelli et al. (2011) and Oriolo et al. (2018); B: Digital elevation model of the same area. The elevation color ramp is limited at 2000 m, but peaks in the highest areas can reach altitudes of up to 2800 m. Note that the limit between high- and low- elevation segments of the continental margin is slightly to the south of the Florianópolis Fracture Zone (location following Torsvik et al., 2009). C: SW-NE topographic cross-section of the study area. The main profile line is approximately parallel to the coast 100 km inland of the shoreline (location in B). Maximum, mean and minimum altitudes along the profile were compiled considering a 25 km buffer to both sides of the main profile line. D and E: Summary of published apatite fission track (AFT) and (U-Th)/He (AHe) ages, respectively, from the Mantiqueira Province and from the margins of neighboring units. Compilation following Oliveira and Jelinek (2017). All references used are listed in section 4.1. AHe ages correspond to average ages from single-crystal results for a same sample. F: Summary of the thermochronological data represented in D and E, according to their position along the cross-section represented in B and C. Filled symbols are located within 25 km of the main profile line, while empty symbols are located within 50 km. Age-dependent color ramp is the same as in D and E, highlighting in more vivid tonalities periods with the majority of the data.

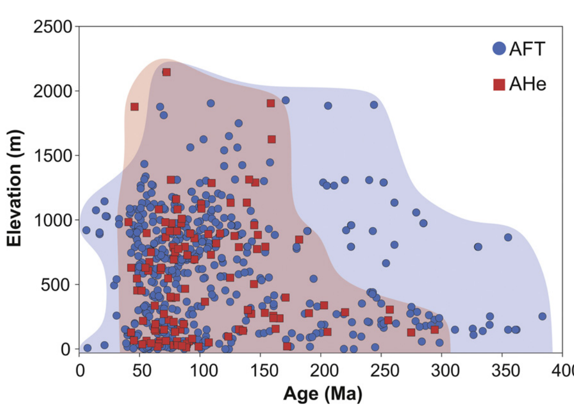

Fig. 10. Distribution of apatite fission-track (AFT) and (U-Th)/He (AHe) ages versus elevation of the corresponding sample. Overlays in blue and red delimit the extension of the AFT and AHe datasets, respectively. Compilation following Oliveira and Jelinek (2017), using the same database as in Fig. 9. (For interpretation of the references to colour in this figure legend, the reader is referred to the web version of this article).

pronounced tectonic activity in the Andean system triggered the reactivation of the inherited Neoproterozoic structures and led to uplift. On the other hand, a different reasoning suggests that the thermal impact of widespread and long-term alkaline magmatism caused extensive exhumation (Cobbold et al., 2001; Hiruma et al., 2010; Cogné et al., 2011, 2012; Karl et al., 2013; Franco-Magalhães et al., 2014; Krob et al., 2019).

In the former hypothesis, the uplift of the passive continental margin would be driven by the far-field contraction in the western margin of the South American Plate, which would also have caused the reactivation of major lineaments inherited from the Brasiliano/Pan-African orogenic cycle (Cobbold et al., 2001; Cogné et al., 2011, 2012; Karl et al., 2013). This reactivation is particularly well illustrated by the development of a number of continental rift basins in the region, including the São Paulo and Taubaté basins (Riccomini et al., 2004). In a sense, this mechanism is in accordance with one of the lines of interpretation of passive margins summarized by Green et al. (2018), which recognize a broad simultaneity between exhumation events in different continents, and therefore suggest that global-scale plate dynamics may play a role in the uplift of continental margins.

In the case of the studied area, however, this hypothesis is contradicted by the new (U-Th)/He results and the integrated

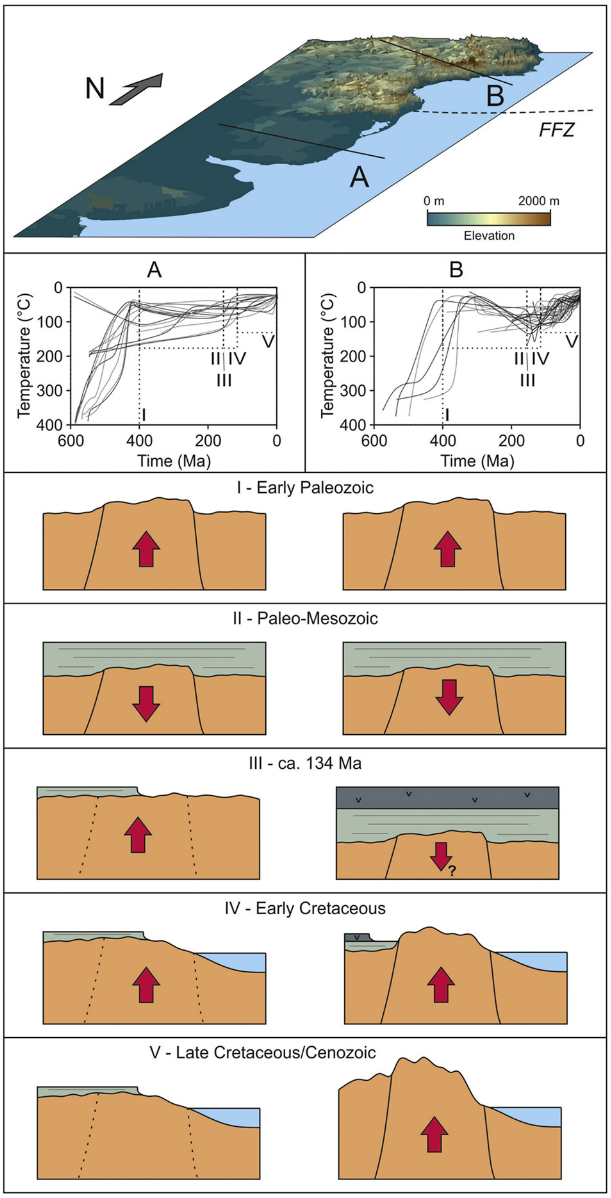

Fig. 11. Schematic evolution of the South American passive margin from the early Paleozoic to the Cenozoic, focusing on the differences between low-elevation (A) and high-elevation (B) portions, as indicated by representative thermal histories published for both sectors (Gallagher et al. (1994); Oliveira et al. (2016a, b), Borba et al. (2002, 2003), Tello Saenz et al. (2003); Franco et al. (2005); Hiruma et al. (2010); Cogné et al. (2012); Karl et al. (2013); Hueck et al., 2017, 2018b, Krob et al. (2019) and this study). Cartoons I to V represent broad regional tendencies, but both areas experienced numerous local variations: I – Early Paleozoic: widespread post-orogenic exhumation; II – Regional subsidence and deposition of the Paraná Basin; III – ca. 134 Ma – Flood volcanism of the Paraná LIP, covering most of southeastern Brazil (B) but with more limited impact in the south (A), which records widespread exhumation; IV – Early Cretaceous: Opening of the South Atlantic ocean and widespread exhumation; V – Late Cretaceous/Cenozoic: Post-rift uplift in Southeast Brazil (B), while the south remained relatively stable, with only limited exhumation. FFZ - Florianópolis Fracture Zone.

thermochronological data compiled in this contribution. If the uplift of the passive margin in southeastern South America was controlled mainly by the interaction between crustal-scale plate tectonic processes and inherited crustal features, the southern portion of the margin, including the Sul-rio-grandense and Uruguayan basement shields, should also have been extensively uplifted, as they share similar structural configurations, with only slight changes in obliquity (Fig. 9A). However, this is not the case. Furthermore, NE-SW structures of the southern Mantiqueira Province seem to have experienced only restricted reactivation, as eventual vertical displacements were insufficient to impact the apatite thermochronological record (Section 3.5; Hueck et al., 2017, 2018b). While the aforementioned slight changes in obliquity might be partially responsible for the different rates of reactivation, such variations are not restricted to the differences between high-and low-elevation sectors of the passive margin. This is exemplified by the uplifted northern extremity of the Mantiqueira Province, in which the main structural features exhibit deflections comparable to those of the southern termination (Fig. 9A).

All this evidence suggests that plate dynamics alone cannot account for the contrast between the contiguous high- and low-elevation segments of the continental margin, and therefore a mantellic process may have been necessary for the uplift of the elevated portions of the passive margin. This has been proposed earlier (e.g., Cobbold et al., 2001; Hiruma et al., 2010; Cogné et al., 2011, 2012), based on the widespread presence of post-rift alkaline magmatism, predominantly concentrated on central and northern portions of the Mantiqueira Province. These intrusive events were interpreted in the past as the result of the drifting of the South American Platform over a mantle plume (Gibson et al., 1995; Thompson et al., 1998). However, the presence of this plume has been somewhat discredited more recently, based on the lack of a correct correlation between geochronological data and the alignment of the main intrusions (Riccomini et al., 2005). Instead, some authors suggest that the post-rift intrusions along the passive margin are controlled mainly by coast-perpendicular NW-SE trending fault systems (Almeida, 1991; Riccomini et al., 2005). Matton and Jébrak (2009) propose that a shallow asthenospheric upwelling, controlled by continental edge-driven mantle flow, would have favored the alkaline magmatism. Such "localized" mantellic mechanisms could, in theory, help sustain elevated margins through long periods of time without a large-scale upwelling (Sacek, 2017). While this association between magmatism and uplift suggests some degree of interconnection, there are still some missing links in the geological record, as the latest exhumation pulses (Paleogene-Neogene) in Southeast Brazil do not correlate with specific magmatic events, while the uplifted plateaus in the Brazilian Northeast do not exhibit significant alkaline intrusions (Riccomini et al., 2005). Nonetheless, it seems at least likely that the same mantle-driven thermal anomaly that fomented the alkaline magmatism in southeastern South America left the central section of the passive margin susceptible to uplift and pronounced fault activity due to thermal weakening (e.g., Cogné et al., 2011, 2012).

In any case, in spite of the complexity of the discussion on the possible causes driving the uplift of the South America passive margin, it seems clear that the reactivation of Neoproterozoic shear zones recognized in elevated regions along the passive margin should be interpreted as a consequence of post-rift uplift, and not a necessary result of plate-scale dynamics. This reactivation could reflect some degree of isostatic compensation due to the regional uplift, which is in accordance with the lack of a direct correlation between individual AFT and AHe ages and sample elevation (Fig. 10). This is not to say that the reactivation of inherited structures did not happen in low-elevation segments, as fault gouge dating and geological observations in the Dom Feliciano Belt suggest recurrent brittle events throughout the Paleo- and Mesozoic (Hueck et al., 2017; Oriolo et al., 2018; Hueck et al. in preparation). In addition, the presence of highly anisotropic lithosphere has traditionally been interpreted to control the rifting that ultimately led to the opening of the South Atlantic Ocean (e.g., Salazar-Mora et al., 2018; Will and Frimmel, 2018). However, at least in the continental onshore of the southern South American passive margin, the lack of extensive uplift means that the reactivation of the inherited structural configuration probably did not cause vertical displacements with enough magnitude to affect the thermochronological record. This may be related with the distance to the active rift axis.

Besides downplaying the impact of the reactivation of the Neoproterozoic shear zones in the exhumation of the South American passive margin, the data compilation instead highlights how transversal structures probably influenced this process. This is exemplified by the remarkable contrasts in apparent ages along the coastline, suggesting a segmentation following NW-SE lineaments. The effect of this structural system is an influential factor in the South American Platform since at least the early Mesozoic, and is not restricted to the exhumation history. It is recorded in the deformation of the Paraná Basin, the emplacement of volcanic dykes during the extrusion of the Paraná-Etendeka LIP, and the segmentation of the passive margin, among others (e.g., Piccirillo et al., 1990; Zalán et al., 1990; Meisling et al., 2001). Its impact in the thermochronological record has also been recognized in South and Southeast Brazil, (Franco-Magalhães et al., 2010; Karl et al., 2013; Krob et al., 2019), and is reflected in the Sul-rio-grandense Shield by the possible reactivation of the Ibaré Shear Zone, the only major Neoproterozoic NW-SE structure in the southern Mantiqueira Province (Fig. 8, section 3.5). The formation of this system has been associated with a clockwise rotation of the South American continent during rifting of the South Atlantic (e.g., Szatmari and Milani, 2016; Salomon et al., 2017), eventually linking to transfer zones of the mid-ocean ridge and the segmentation of the oceanic crust (Cobbold et al., 2001; Torsvik et al., 2009; Stica et al., 2014). In fact, the limit between post-rift uplifted segments of the passive margin and low-elevation areas characterized by pre- to syn-rift apparent ages broadly coincides with the location of the Florianópolis Fracture Zone. This structure, one of the principal transversal structures in the South Atlantic (e.g., Torsvik et al., 2009), is located slightly to the south of the southernmost extension of the elevated plateaus along the South American passive margin (Figs. 1,9). In this sense, the impact of this structure in the segmentation of the South American Plate may have influenced the localization of the mantellic processes that are hypothesized to have influenced the passive margin uplift and associated alkaline magmatism, such as the restricted asthenospheric upwelling (Matton and Jébrak, 2009).

5. Conclusions

Despite constituting a fundamental feature of plate tectonics, elementary questions on the geodynamics of passive margins remain controversial. The mechanisms by which continental margins may be uplifted, its relation to continental rifting and break-up and the influence of lithospheric and mantellic processes are still a matter of debate, complicated by the fact that many marginal segments are not elevated at all. These questions were addressed here using new and compiled thermochronological data. The new (U-Th)/He dataset reveals a complex and multi-stage exhumation history for a low-elevation segment of the South American passive margin in southern Brazil. Modelled thermal histories suggest extensive post-orogenic exhumation in the early Paleozoic, followed by exposure to near-surface conditions and burial by sediments up until the Mesozoic. Final exhumation of most of the Sul-rio-grandense Shield was achieved at the latest during the rifting and opening of the South Atlantic Ocean, and in some samples hundreds of millions of years earlier. While block tectonics probably played an important role throughout its evolution, the only shear zone in the Sul-rio-grandense Shield that seems to have impacted the thermochronological record has a structural configuration (NW-SE) transversal to the main structural grain. A compilation of apatite fission-track and (U-Th)/He data between eastern Argentina and eastern Brazil reveals that, in spite of sharing a similar structural configuration, the South American continental margin along the Mantiqueira Province exhibits contrasting exhumation histories. High-elevation segments of the coastline were extensively exhumed after the continental break-up, while low-elevation segments record almost exclusively pre-rifting events. The contrast between both styles of the South American passive margin cannot be explained only by the interaction of the inherited structures and plate dynamics, suggesting that mantellic processes may have had an impact in its evolution as well. These processes would also be associated with the intrusion of post-rift alkaline magmatism, and could have contributed to more pronounced fault reactivation in elevated areas of East Brazil. The contrast exhibited along the continental margin also evidences the impact of important oceanic fracture zones, as the separation between both portions of the passive margin is coast-perpendicular and located slightly to the north of the Florianópolis Transfer Zone.

Acknowledgements

M. Hueck thanks the CNPq for a PhD scholarship in Germany within the Science Without Borders Program. M.A.S. Basei and M. Hueck thank FAPESP for funding from the Thematic Project 2015/03737-0. Sampling in the Sul-rio-grandense Shield was immensely aided by the generous help of Ruy P. Philipp. David Hindle is thanked for the DEM of Fig. 1. We would also like to thank two anonymous reviewers and editor Philippe Agard for thoughtful and constructive comments that helped improve this manuscript.

Appendices A to E. Supplementary data

Supplementary material related to this article can be found, in the online version, at http://dx.doi.org/10.1016/j.tecto.2019.228222.

References

Ab'Sáber, A.N., 2000. Summit surfaces in Brazil. Revista Brasileira de Geociências 30 (3), 515–516.
Almeida, F.F.M., Hasui, Y., de Brito Neves, B.B., Fuck, R.A., 1981. Brazilian structural provinces; an introduction. Earth-Sci. Rev. 17 (1/2), 1–29.
Almeida, F.F.M., 1991. O alinhamento magmatico de Cabo Frio. 2° Simposio de Geologia do Sudeste, Sao Paulo. Abstracts. pp. 423–428.
Almeida, R.P., Santos, M.G.M., Fragoso-Cesar, A.R., Janikian, L., Fambrini, G.L., 2012. Recurring extensional and strike-slip tectonics after the Neoproterozoic collisional events in the southern Mantiqueira province. Ann. Braz. Acad. Sci. 84 (2), 347–376.
Assine, M.L., Soares, P.C., Milani, E.J., 1994. Sequências tectono-sedimentares mesopaleozóicas da Bacia do Paraná, Sul do Brasil. Revista Brasileira de Geociências 24 (2), 77–89.
Ault, A.K., Flowers, R.M., 2012. Is apatite U–Th zonation information necessary for accurate interpretation of apatite (U–Th)/He thermochronometry data? Geochimica et Cosmochimica Acta 79, 60–78.
Ault, A.K., Flowers, R.M., Bowring, S.A., 2009. Phanerozoic burial and unroofing history of the western Slave craton and Wopmay orogen from apatite (U–Th)/He thermochronometry. Earth Planet. Sci. Lett. 284 (1), 1–11.
Babinski, M., Chemale, F., Hartmann, L.A., Van Schmus, W.R., da Silva, L.C., 1997. U-Pb and Sm-Nd geochronology of the Neoproterozoic granitic-gneissic Dom Feliciano belt, southern Brazil. J. South Am. Earth Sci. 10 (3–4), 263–274.
Basei, M.A.S., Siga Jr., O., Masquelin, H., Harara, O.M., Reis Neto, J.M., Preciozzi, F., 2000. In: Cordani, U.G., Milani, E.J., Thomaz Filho, A., Campos, D.A. (Eds.), The Dom Feliciano Belt of Brazil and Uruguay and its Foreland Domain the Rio de la Plata Craton: Framework, Tectonic Evolution and Correlation With Similar Provinces of Southwestern Africa. Tectonic Evolution of South America, IGC 31, Rio de Janeiro, pp. 311–334.
Basei, M.A.S., Frimmel, H.E., Nutman, A.P., Preciozzi, F., Jacob, J., 2005. The connection between the Neoproterozoic Dom Feliciano (Brazil/Uruguay) and Gariep (Namibia/South Africa) orogenic belts. Precambrian Res. 139, 139–221.
Basei, M.A.S., Frimmel, H.E., Nutman, A.P., Preciozzi, F., 2008. West gondwana amalgamation based on detrital zircon ages from neoproterozoic Ribeira and Dom Feliciano belts of South America and comparison with coeval sequences from SW Africa. In: In: Pankhurst, R.J., Trouw, R.A.J., de Brito Neves, B.B., de Wit, M.J. (Eds.), West Gondwana: Pre-Cenozoic Correlations Across the South Atlantic Region 294. Geological Society London, Special Publication, London, pp. 239–256.
Basei, M.A.S., Neves, B.B.B., Junior, O.S., Babinski, M., Pimentel, M.M., Tassinari, C.C.G., Hollanda, M.H.B., Nutman, A., Cordani, U.G., 2010. Contribution of SHRIMP U–Pb zircon geochronology to unravelling the evolution of Brazilian Neoproterozoic fold belts. Precambrian Res. 183 (1), 112–144.
Basei, M.A.S., Frimmel, H., Campos Neto, M.C., Araújo, C.A., Castro, N.A., Passarelli, C.R., 2018. The tectonic history of the Southern adamastor Ocean based on a correlation of the Kaoko and Dom Feliciano Belts. In: Siegesmund, S., Oyhantçabal, P., Basei, M.A.S., Oriolo, S. (Eds.), Geology of Southwest Gondwana. Regional Geology Reviews. Springer, Heidelberg, pp. 63–85.
Bicca, M.M., Chemale Jr, F., Jelinek, A.R., Oliveira, C.H.E., Guadagnin, F., Armstrong, R., 2013. Tectonic evolution and provenance of the santa bárbara group, camaquã mines region, Rio Grande do sul, Brazil. J. South Am. Earth Sci. 48, 173–192.
Borba, A.W., Vignol-Lelarge, M.L.M., Mizusaki, A.M.P., 2002. Uplift and denudation of the Caçapava do Sul granitoids (southern Brazil) during Late Paleozoic and Mesozoic:

constraints from apatite fission-track data. J. South Am. Earth Sci. 15 (2), 683–692.
Borba, A.W., Lima, E.F., Vignol-Lelarge, M.L.M., Mizusaki, A.M.P., Sparrenberg, I., Barros, C.E., 2003. Significance of Late Paleozoic fission-track ages in volcanic rocks from the Lavras do Sul region, southernmost Brazil. Gondwana Res. 6 (1), 79–88.
Borba, A.W., Mizusaki, A.M.P., Silva, D.R.A., Noronha, F.L., Casagrande, J., 2006. Provenance of the Neoproterozoic Maricá Formation (Sul-rio-grandense Shield, Southern Brazil): petrographic and Sm- Nd isotopic constrains. Gondwana Res. 9, 464–474.
Brito Neves, B.B., Fuck, R.A., 2014. The basement of the South American platform: half Laurentian (N-NW) + half Gondwanan (E-SE) domains. Precambrian Res. 244, 75–86.
Chery, J., Lucazeau, F., Daignieres, M., Vilotte, J.P., 1992. Large uplift of rift flanks: a genetic link with lithospheric rigidity? Earth Planet. Sci. Lett. 112 (1–4), 195–211.
Cañón-Tapia, E., 2018. The Paraná-Etendeka Continental Flood Basalt Province: a historical perspective of current knowledge and future research trends. J. Volcanol. Geotherm. Res. 355, 287–303.
Cobbold, P.R., Meisling, K.E., Mount, V.S., 2001. Reactivation of an obliquely rifted margin, Campos and santos basins, Southeastern Brazil. Bull. 85, 1925–1944.
Cogné, N., Gallagher, K., Cobbold, P.R., 2011. Post-rift reactivation of the onshore margin of southeast Brazil: evidence from apatite (U–Th)/He and fission-track data. Earth Planet. Sci. Lett. 309, 118–130.
Cogné, N., Gallagher, K., Cobbold, P.R., Riccomini, C., Gautheron, C., 2012. Post-breakup tectonics in southeast Brazil from thermochronological data and combined inverse-forward thermal history modelling. Journal of Geophysical Research B: Solid Earth 117 (11). https://doi.org/10.1029/2012JB009340.
Contreras, J., Zühlke, R., Bowman, S., Bechstädt, T., 2010. Seismic stratigraphy and subsidence analysis of the southern Brazilian margin (Campos, Santos and Pelotas basins). Mar. Pet. Geol. 27 (9), 1952–1980.
Demoulin, A., Zarate, M., Rabassa, J., 2005. Long-term landscape development: a perspective from the southern Buenos Aires ranges of east central Argentina. J. South Am. Earth Sci. 19 1963-204.
Egydio-Silva, M., Vauchez, A., Fossen, H., Cavalcante, G.C.G., Xavier, B.C., 2018. Connecting the Araçuaí and Ribeira belts (SE–brazil): progressive transition from contractional to transpressive strain regime during the Brasiliano orogeny. J. South Am. Earth Sci. 86, 127–139.
Fernandes, L.A.D., Tommasi, A., Porcher, C.C., 1992. Deformation patterns in the southern brazilian branch of the Dom Feliciano Belt: a reappraisal. J. South Am. Earth Sci. 5, 77–96.
Florisbal, L.M., Heaman, L.M., de Assis Janasi, V., Bitencourt, M.F., 2014. Tectonic significance of the Florianópolis Dyke Swarm, Paraná–Etendeka Magmatic Province: A reappraisal based on precise U–Pb dating. J. Volcanol. Geotherm. Res. 289, 140–150.
Flowers, R.M., Kelley, S.A., 2011. Interpreting data dispersion and inverted dates in apatite (U–Th)/He and fission-track datasets: an example from the U.S. Mid-continent. Geochim. Cosmochim. Acta 75 (18), 5169–5186.
Flowers, R., Ketcham, R.A., Shuster, D.L., Farley, K.A., 2009. Apatite (U–Th)/He thermochronometry using a radiation damage accumulation and annealing model. Geochim. Cosmochim. Acta 73, 2347–2365.
Franco, A.O.B., Hackspacher, P.C., Godoy, D.F., Ribeiro, L.F.B., Guedes, S., 2005. História térmica do Maciço Alcalino de Poços de Caldas (SP/MG) e adjacências através da análise de datação por traços de fissão em apatitas. Revista Brasileira de Geociências 35 (3), 351–358.
Franco-Magalhães, A.O.B., Hackspacher, P.C., Glasmacher, U.A., Saad, A.R., 2010. Rift to post-rift evolution of a '"passive"' continental margin: the Ponta Grossa Arch, SE Brazil. Int. J. Earth Sci. 99, 1599–1613.
Franco-Magalhães, A.O.B., Cuglieri, M.A.A., Hackspacher, P.C., Saad, A.R., 2014. Long-term landscape evolution and post-rift reactivation in the southeastern Brazilian passive continental margin: taubaté basin. Int. J. Earth Sci. 103, 441–453.
Gallagher, K., Hawkesworth, C.J., Mantovani, M.S.M., 1994. The denudation history of the onshore continental margin of SE Brazil inferred from apatite fission track data. J. Geophys. Res. Solid Earth 99 (B9), 18117–18145.
Gautheron, C., Barbarand, J., Ketcham, R.A., Tassan-Got, L., van der Beek, P., Pagel, M., Pinna-Jamme, R., Couffignal, F., Fialin, M., 2013. Chemical influence on α-recoil damage annealing in apatite: implications for (U–Th)/He dating. Chem. Geol. 351, 257–267.
Gibson, S.A., Thompson, R.N., Leonardos, O.H., Dickin, A.P., Mitchell, J.G., 1995. The Late Cretaceous impact of the Trindade mantle plume: evidence from large-volume, mafic, potassic magmatism in SE Brazil. J. Petrol. 36 (1), 189–229.
Gilchrist, A.R., Summerfield, M.A., 1990. Differential denudation and flexural isostacy in formation of rifted-margin upwarps. Nature 346 (6286), 739.
Gomes, C.H., Almeida, D., 2019. New insights into the Gondwana breakup at the Southern South America by apatite fission-track analyses. Adv. Geosci. 47, 1–15.
Green, P., Duddy, I., 2018. Apatite (U-Th-Sm)/He thermochronology on the wrong side of the tracks. Chem. Geol. 488, 21–33.
Green, P.F., Japsen, P., Chalmers, J.A., Bonow, J.M., Duddy, I.R., 2018. Post-breakup burial and exhumation of passive continental margins: seven propositions to inform geodynamic models. Gondwana Res. 53, 58–81.
Guenthner, W.R., Reiners, P.W., Ketcham, R.A., Nasdala, L., Giester, G., 2013. Helium diffusion in natural zircon: radiation damage, anisotropy, and the interpretation of zircon (U-Th)/He thermochronology. Am. J. Sci. 313, 145–198.
Guenthner, W.R., Reiners, P.W., Drake, H., Tillberg, M., 2017. Zircon, titanite, and apatite (U-Th)/He ages and age-eU correlations from the Fennoscandian Shield, southern Sweden. Tectonics 36, 1254–1274.
Hackspacher, P.C., Ribeiro, L.F.B., Ribeiro, M.C.S., Fetter, A.H., Hadler Neto, J.C., Tello Saenz, C.A., Dantas, E.L., 2004. Consolidation and break-up of the South American platform in southeastern Brazil: tectonothermal and denudation histories. Gondwana Res. 1, 91–101.
Hackspacher, P.C., Godoy, D.F., Ribeiro, L.F.B., Neto, J.C.H., Franco, A.O.B., 2007. Modelagem térmica e geomorfologia da borda sul do Cráton do São Francisco: termocronologia por traços de fissão em apatita. Revista Brasileira de Geociências 37 (4), 76–86.
Harrison, T.M., Célérier, J., Aikman, A.B., Hermann, J., Heizler, M.T., 2009. Diffusion of 40Ar in muscovite. Geochim. Cosmochim. Acta 73, 1039–1051.
Hartmann, L.A., Chemale Jr., F., 2003. Mid amphibolite facies metamorphism of harzburgites in the Neoproterozoic Cerro Mantiqueiras Ophiolite, southernmost Brazil. Anais da Academia Brasileira de Ciências 75 (1), 109–128.
Hartmann, L.A., Philipp, R.P., Santos, J.O.S., McNaughton, N.J., 2011. Time frame of 753-680 Ma juvenile accretion during the São Gabriel orogeny, southern Brazil. Gondwana Res. 19, 84–99.
Heilbron, M., Valeriano, C.M., Tassinari, C.C.G., Almeida, J., Tupinambá, M., Siga, O., Trouw, R., 2008. Correlation of Neoproterozoic terranes between the Ribeira Belt, SE Brazil and its African counterpart: comparative tectonic evolution and open questions. Geol. Soc. London Spec. Publ. 294 (1), 211–237.
Hiruma, S.T., Riccomini, C., Modenesi-Gauttieri, M.C., Hackspacher, P.C., Hadler Neto, J.C., Franco-Magalhães, A.O.B., 2010. Denudation history of the Bocaina Plateau, Serra do Mar, Southeastern Brazil: relationships to Gondwana breakup and passive margin development. Gondwana Res. 18, 674–687.
Holz, M., Küchle, J., Philipp, R.P., Bischoff, A.P., Arima, N., 2006. Hierarchy of tectonic control on stratigraphic signatures: base-level changes during the early Permian in the Paraná Basin, southernmost Brazil. J. South Am. Earth Sci. 22 (3), 185–204.
Hueck, M., Oriolo, S., Dunkl, I., Wemmer, K., Oyhantçabal, P., Schanofski, M., Basei, M.A.S., Siegesmund, S., 2017. Phanerozoic low-temperature evolution of the Uruguayan Shield along the South American passive margin. Journal of the Geological Society of London 174, 609–626.
Hueck, M., Oyhantçabal, P., Philipp, R.P., Basei, M.A.S., Siegesmund, S., 2018a. The Dom Feliciano Belt in Southern Brazil and Uruguay. In: Siegesmund, S., Oyhantçabal, P., Basei, M.A.S., Oriolo, S. (Eds.), Geology of Southwest Gondwana. Regional Geology Reviews. Springer, Heidelberg, pp. 267–302.
Hueck, M., Dunkl, I., Heller, B., Stipp Basei, M.A., Siegesmund, S., 2018b. (U-Th)/He Thermochronology and Zircon Radiation Damage in the South American Passive Margin: Thermal Overprint of the Paraná LIP? Tectonics 37 (10), 4068–4085.
Hueck, M., Basei, M.A.S., Wemmer, K., Oriolo, S., Heidelbach, F., Siegesmund, S., 2018c. Evolution of the major Gercino Shear Zone in the Dom Feliciano Belt, South Brazil, and implications for the assembly of southwestern Gondwana. Int. J. Earth Sci. https://doi.org/10.1007/s00531-018-1660-4.
Janasi, V.A., Freitas, V.A., Heaman, L.H., 2011. The onset of flood basalt volcanism, Northern Paraná Basin, Brazil: a precise U–Pb baddeleyite/zircon age for a Chapecó-type dacite. Earth Planet. Sci. Lett. 302, 147–153.
Janikian, L., Almeida, R.P., Fragoso-Cesar, A.R.S., Martins, V.T.S., Dantas, E.L., Tohver, E., Mc Reath, I., D'Agrella Filho, M.S., 2012. Ages (U-Pb SHRIMP and LA-ICP-MS) and stratigraphic evolution of the Neoproterozoic volcano-sedimentary successions from extensional Camaquã Basin, Southern Brazil. Gondwana Res. 21, 466–482.
Japsen, P., Chalmers, J.A., Green, P.F., Bonow, J.M., 2012. Elevated, passive continental margins: not rift shoulders, but expressions of episodic, post-rift burial and exhumation. Glob. Planet. Change 90, 73–86.
Jelinek, A.R., Neto, A.C.B., Poupeau, G., 2003. Análise por traços de fissão em apatitas do Distrito Fluorítico de Santa Catarina: relações entre hidrotermalismo e evolução da margem continental. Revista Brasileira de Geociências 33 (3), 289–298.
Jelinek, A.R., Chemale Jr., F.C., van der Beek, P.A., Guadagnin, F., Cupertino, J.A., Viana, A., 2014. Denudation history and landscape evolution of the northern East-Brazilian continental margin from apatite fission-track thermochronology. J. South Am. Earth Sci. 54, 158–181.
Johnson, J.E., Flowers, R.M., Baird, G.B., Mahan, K.H., 2017. "Inverted" zircon and apatite (U–Th)/He dates from the Front Range, Colorado: high-damage zircon as a low-temperature (< 50∘C) thermochronometer. Earth Planet. Earth Sci. 466, 80–90.
Karl, M., Glasmacher, U.A., Kollenz, S., Franco-Magalhães, A.O.B., Stockli, D.F., Hackspacher, P.C., 2013. Evolution of the South Atlantic passive continental margin in southern Brazil derived from zircon and apatite (U–Th–Sm)/He and fission-track data. Tectonophysics 604, 224–244.
Ketcham, R.A., 2005. Forward and inverse modeling of low-temperature thermochronometry data. Rev. Mineral. Geochem. 58 (1), 275–314.
Ketcham, R.A., Gautheron, C., Tassan-Got, L., 2011. Accounting for long alpha-particle stopping distances in (U–Th–Sm)/He geochronology: refinement of the baseline case. Geochimica et Cosmologica Acta 75, 7779–7791.
Kollenz, S., 2015. Long-term Landscape Evolution, Cooling and Exhumation History of the South American Passive Continental Margin in NE Argentina & SW Uruguay. Phd Thesis. Ruprecht-Karls-Universität Heidelberg.
Kollenz, S., Glasmacher, U.A., Rossello, E.A., Stockli, D.F., Schad, S., Pereyra, R.E., 2016. Thermochronological constraints on the Cambrian to recent geological evolution of the Argentina passive continental margin. Tectonophysics 716, 182–203.
Krob, F.C., Glasmacher, U.A., Karl, M., Perner, M., Hackspacher, P.C., Stockli, D.F., 2019. Multi-chronometer thermochronological modelling of the Late Neoproterozoic to recent tT-evolution of the SE coastal region of Brazil. J. South Am. Earth Sci. 92, 77–94.
Lena, L.O.F., Pimentel, M.M., Philipp, R.P., Armstrong, R., Sato, K., 2014. The evolution of the Neoproterozoic São Gabriel juvenile terrane, southern Brazil based on high spatial resolution U-Pb ages and 18O data from detrital zircons. Precambrian Res. 247, 126–138.
López-Gamundi, O.R., Rosello, E.A., 1993. Devonian-Carboniferous unconformity in Argentina and its relation to the Eo-Hercynian orogeny in southern South America. Geol. Rundschau 82, 136–147.
Malusà, M.G., Carter, A., Limoncelli, M., Villa, I.M., Garzanti, E., 2013. Bias in detrital zircon geochronology and thermochronometry. Chem. Geol. 359, 90–107.

Matton, G., Jébrak, M., 2009. The Cretaceous Peri-Atlantic Alkaline Pulse (PAAP): deep mantle plume origin or shallow lithospheric break-up? Tectonophysics 469 (1-4), 1–12.

McDannell, K.T., Zeitler, P.K., Janes, D.G., Idleman, B.D., Fayon, A.K., 2018. Screening apatites for (U-Th)/He thermochronometry via continuous ramped heating: He age components and implications for age dispersion. Geochim. Cosmochim. Acta 223, 90–106.

Meisling, K.E., Cobbold, P.R., Mount, V.S., 2001. Segmentation of an obliquely rifted margin, Campos and santos basins, Southeastern Brazil. Bull. 85 (11), 1903–1924.

Milani, E.J., Melo, J.H.G., Souza, P.A., Fernandes, L.A., França, A.B., 2007. Bacia do Paraná. In: Milani, E.J., Rangel, H.D., Bueno, G.V., Stica, J.M., Winter, W.R., Caixeta, J.M., Pessoa Neto, O.C. (Eds.), Bacias Sedimentares Brasileiras – Cartas Estratigráficas: Boletim de Geociências da Petrobras, 15, Rio de Janeiro.

Moulin, M., Aslanian, D., Unternehr, P., 2010. A new starting point for the South and Equatorial Atlantic Ocean. Earth-Sci. Rev. 98 (1–2), 1–37.

Nasdala, L., Wenzel, M., Vavra, G., Irmer, G., Wenzel, T., Kober, B., 2001. Metamictisation of natural zircon: accumulation versus thermal annealing of radioactivity-induced damage. Contrib. Mineral. Petrol. 141, 125–144.

Nielsen, S.B., Gallagher, K., Leighton, C., Balling, N., Svenningsen, L., Jacobsen, B.H., et al., 2009. The evolution of western Scandinavian topography: a review of Neogene uplift versus the ICE (isostasy–climate–erosion) hypothesis. J. Geodyn. 47 (2–3), 72–95.

Oliveira, C.H.E., Jelinek, A.R., 2017. História termotectônica da margem continental brasileira a partir de dados de traços de fissão em apatita. Pesquisas em Geociências 44 (3), 387–400.

Oliveira, C.H.E., Jelinek, A.R., Chemale Jr., F., Bernet, M., 2016a. Evidence of post-Gondwana breakup in Southern Brazilian Shield: insights from apatite and zircon fission track thermochronology. Tectonophysics 666, 173–187.

Oliveira, C.H.E., Jelinek, A.R., Chemale Jr, F., Cupertino, J.A., 2016b. Thermotectonic history of the southeastern Brazilian margin: evidence from apatite fission track data of the offshore Santos Basin and continental basement. Tectonophysics 685, 21–34.

Oliveira, S.G., Hackspacher, P.C., Neto, J.C.H., Iunes, P.J., de Paulo, S.R., Ribeiro, L.F.B., Tello-Saenz, C.A., 2000. Constraints on the evolution and thermal history of the continental platform of southeast Brazil, Sao Paulo State, using apatite fission track analysis (AFTA). Revista Brasileira de Geociências 30 (1), 107–109.

Oriolo, S., Oyhantçabal, P., Wemmer, K., Heidelbach, F., Pfänder, J., Basei, M.A.S., Hueck, M., Hannich, F., Sperner, B., Siegesmund, S., 2016a. Shear zone evolution and timing of deformation in the Neoproterozoic transpressional Dom Feliciano Belt. Uruguay. Journal of Structural Geology 92, 59–78.

Oriolo, S., Oyhantçabal, P., Basei, M.A.S., Wemmer, K., Siegesmund, S., 2016b. The Nico Pérez Terrane (Uruguay): from Archean crustal growth and connections with the Congo Craton to late Neoproterozoic accretion to the Río de la Plata Craton. Precambrian Res. 280, 147–160.

Oriolo, S., Hueck, M., Oyhantçabal, P., Goscombe, B., Wemmer, K., Siegesmund, S., 2018. Shear zones in Brasiliano-Pan-African belts and their role in the amalgamation and break-Up of Southwest Gondwana. In: Siegesmund, S., Oyhantçabal, P., Basei, M.A.S., Oriolo, S. (Eds.), Geology of Southwest Gondwana. Regional Geology Reviews. Springer, Heidelberg, pp. 593–613.

Orme, D.A., Reiners, P.W., Hourigan, J.K., Carrapa, B., 2015. Effects of inherited cores and magmatic overgrowths on zircon (U-Th)/He ages and age-eU trends from Greater Himalayan sequence rocks, Mount Everest region. Tibet. Geochemistry, Geophysics, Geosystems 16 (8), 2499–2507.

Oyhantçabal, P., Siegesmund, S., Wemmer, K., Presnyakov, S., Layer, P., 2009. Geochronological constraints on the evolution of the southern Dom Feliciano Belt (Uruguay). Journal of the Geological Society of London 166, 1075–1084.

Oyhantçabal, P., Oriolo, S., Philipp, R.P., Wemmer, K., Siegesmund, S., 2018. The Nico Pérez Terrane of Uruguay and Southeastern Brazil. In: Siegesmund, S., Oyhantçabal, P., Basei, M.A.S., Oriolo, S. (Eds.), Geology of Southwest Gondwana. Regional Geology Reviews. Springer, Heidelberg, pp. 161–188.

Palenik, C.S., Nasdala, L., Ewing, R.C., 2003. Radiation damage in zircon. Am. Mineral. 88 (5–6), 770–781.

Panario, D., Gutiérrez, O., Sánchez-Betucci, L., Peel, E., Oyhantçabal, P., Rabassa, J., 2014. Ancient landscapes of Uruguay. In: Rabassa, J., Ollier, C. (Eds.), Gondwana Landscapes in Southern South America. Springer.

Passarelli, C.R., Basei, M.A.S., Wemmer, K., Siga Jr., O., Oyhantçabal, P., 2011. Major Shear Zones of southern Brazil and Uruguay: escape tectonics in the eastern border of Rio de La Plata and Paranapanema cratons during the Western Gondwana amalgamation. International Journal of Earth Sciences (Geol.Rundsch) 100, 391–414.

Pertille, J., Hartmann, L.A., Santos, J.O.S., McNaughton, N.J., Armstrong, R., 2017. Reconstructing the Cryogenian–Ediacaran evolution of the Porongos fold and thrust belt, Southern Brasiliano Orogen, based on Zircon U–Pb–Hf–O isotopes. Int. Geol. Rev. 59 (12), 1532–1560.

Philipp, R.P., Machado, R., 2005. The Neoproterozoic to Cambrian granitic magmatism of the pelotas batholith, southern Brazil. Journal of South American Earth Science 19, 461–478.

Philipp, R.P., Machado, R., Chemale Jr., F., 2003. Reavaliação e novos dados geocronológicos (Ar/Ar, Rb/Sr e Sm/Nd) do Batólito Pelotas no Rio Grande do Sul: implicações petrogenéticas e idade de reativação das zonas de cisalhamento. Geologia USP, Série Científica 3, 71–84.

Philipp, R.P., Pimentel, M.M., Chemale Jr., F., 2016. Tectonic evolution of the Dom Feliciano Belt in Southern Brazil: geological relationships and U-Pb geochronology. Braz. J. Geol. 46 (1), 83–104.

Philipp, R.P., Pimentel, M.M., Basei, M.A.S., 2018. the tectonic evolution of the São Gabriel Terrane, Dom Feliciano Belt, Southern Brazil: the closure of the charrua Ocean. In: Siegesmund, S., Oyhantçabal, P., Basei, M.A.S., Oriolo, S. (Eds.), Geology of Southwest Gondwana. Regional Geology Reviews. Springer, Heidelberg, pp. 243–265.

Piccirillo, E.M., Bellieni, G., Cavazzini, G., Comin-Chiaramonti, P., Petrini, R., Melfi, A.J., Pinese, J.P.P., Zantadeschi, P., De Min, A., 1990. Lower Cretaceous tholeiitic dyke swarms from the Ponta Grossa Arch (southeast Brazil): Petrology, Sr-Nd isotopes and genetic relationships with the Paraná flood volcanics. Chem. Geol. 89 (1–2), 19–48.

Pinto, V.M., Hartmann, L.A., Santos, J.O.S., McNaughton, N.J., Wildner, W., 2011. Zircon UPb geochronology from the Paraná bimodal volcanic province support a brief eruptive cycle at ∼135 Ma. Chem. Geol. 281 (1–2), 93–102.

Purdy, J.W., Jäger, E., 1976. K-Ar ages on rock-forming minerals from the Central Alps. Memorie degli Istituti di Geologia e Mineralogia dell'Università di Padova 30, 1–31.

Renne, P.R., Ernesto, M., Pacca, I.G., Coe, R.S., Glen, J.M., Prévot, M., Perrin, M., 1992. The age of ParanJ flood volcanism, rifting of Gondwanaland, and the jurassic-cretaceous boundary. Science 258, 975–979.

Rossetti, L., Lima, E.F., Waichel, B.L., Hole, M.J., Simões, M.S., Scherer, C.M., 2018. Lithostratigraphy and volcanology of the Serra Geral Group, Paraná-Etendeka Igneous Province in southern Brazil: towards a formal stratigraphical framework. J. Volcanol. Geotherm. Res. 355, 98–114.

Ribeiro, L.F.B., Hackspacher, P.C., Ribeiro, M.C.S., Hadler Neto, J.C., Tello, S.C.A., Iunes, P.J., Franco, A.O.B., Godoy, D.F., 2005. Thermotectonic and fault dynamic analysis of Precambrian basement and tectonic constraints with the Parana basin. Radiat. Meas. 39, 669–673.

Riccomini, C., 1997. Arcabouço estrutural e aspectos do tectonismo gerador e deformador da Bacia Bauru no Estado de São Paulo. Revista Brasileira de Geociências 27 (2), 153–162.

Riccomini, C., Sant'Anna, L.G., Ferrari, A.L., 2004. Evolução geológica do rift continental do sudeste do Brasil. In: Mantesso-Neto, V., Bartorelli, A., Carneiro, C.D.R., Brito-Neves, B.D. (Eds.), Geologia do continente Sul-Americano: evolução da obra de Fernando Flávio Marques de Almeida, Beca, São Paulo, pp. 383–405.

Riccomini, C., Velázquez, V.F., Gomes, C.B., 2005. Tectonic controls of the Mesozoic and Cenozoic alkaline magmatism in central-southeastern Brazilian Platform. Mesozoic to Cenozoic alkaline magmatism in the Brazilian Platform 123, 31–56.

Rocha-Campos, A.C., Basei, M.A.S., Nutman, A.P., Santos, P.R., Passarelli, C.R., Canile, F.M., Rosa, O.C., Fernandes, M.T., Santa Ana, H., Veroslavsky, G., 2019. U-Pb zircon dating of ash fall deposits from the Paleozoic Paraná Basin of Brazil and Uruguay: a reevaluation of the stratigraphic correlations. J. Geol. 127 (2) 000-000.

Saalmann, K., Gerdes, A., Lahaye, Y., Hartmann, L.A., Remus, M.V.D., Läufer, A., 2011. Multiple accretion at the eastern margin of the Rio de la Plata craton: the prolonged Brasiliano orogeny in southernmost Brazil. Int. J. Earth Sci. 100, 355–378.

Sacek, V., 2017. Post-rift influence of small-scale convection on the landscape evolution at divergent continental margins. Earth Planet. Sci. Lett. 459, 48–57.

Sacek, V., Braun, J., Van der Beek, P., 2012. The influence of rifting on escarpment migration on high elevation passive continental margins. J. Geophys. Res. Solid Earth 117 (B04407). https://doi.org/10.1029/2011JB008547.

Salazar-Mora, C.A., Huismans, R.S., Fossen, H., Egydio-Silva, M., 2018. The Wilson cycle and effects of tectonic structural inheritance on rifted passive margin formation. Tectonics 37 (9), 3085–3101.

Salomon, E., Passchier, C., Koehn, D., 2017. Asymmetric continental deformation during South Atlantic rifting along southern Brazil and Namibia. Gondwana Res. 51, 170–176.

Siegesmund, S., Oyhantçabal, P., Basei, M.A.S., Oriolo, S., 2018. Geology of Southwest Gondwana. Regional Geology Reviews. Springer, Heidelberg.

Silva, L.C., Hartmann, L.A., McNaughton, N.J., Fletcher, I.R., 1997. SHRIMP U/Pb zircon dating of Neoproterozoic granitic magmatism and collision in the Pelotas batholith, southernmost Brazil. Int. Geol. Rev. 41, 531–551.

Silva, Z.C.C., Cornford, C., 1985. The kerogen type, depositional environment and maturity, of the lrati Shale, Upper Permian of Paraná Basin, Southern Brazil. Organic Geochemestry 8 (6), 399–411.

Souza, D.H., Hackspacher, P.C., Doranti-Tiritan, C., Godoy, D.F., 2014. Comparação da dinâmica evolutiva, em longo e curto prazo, entre o Planalto de Poços de Caldas e o Planalto de São Pedro de Caldas. Rev. Bras. Geomorfol. 16 (2), 251–272.

Spiegel, C., Kohn, B., Belton, D., Berner, Z., Gleadow, A., 2009. Apatite (U–Th–Sm)/He thermochronology of rapidly cooled samples: the effect of He implantation. Earth Planet. Sci. Lett. 285 (1), 105–114.

Stica, J.M., Zalán, P.V., Ferrari, A.L., 2014. The evolution of rifting on the volcanic margin of the Pelotas Basin and the contextualization of the Paraná-Etendeka LIP in the separation of Gondwana in the South Atlantic. Mar. Pet. Geol. 50, 1–21.

Szatmari, P., Milani, E.J., 2016. Tectonic control of the oil-rich large igneous-carbonate-salt province of the South Atlantic rift. Marine And Petroleum Geolog 77, 567–596.

Tello Saenz, C.A., Hackspacher, P.C., Hadler, N.J.C., Iunes, P.J., Guedes, S., Paulo, S.R., Ribeiro, L.F.B., 2003. Recognition of cretaceous, Paleocene and Neogene tectonic reactivation, through apatite fission-track analysis in Precambrian areas of the Southeast Brazil: association with the South Atlantic Ocean Opening. J. South Am. Earth Sci. 15, 137–142.

Thiede, D.S., Vasconcelos, P.M., 2010. Parana flood basalts: rapid extrusion hypothesis confirmed by new 40Ar/39Ar results. Geology 38 (8), 747–750.

Thompson, R.N., Gibson, S.A., Mitchell, J.G., Dickin, A.P., Leonardos, O.H., Brod, J.A., Greenwood, J.C., 1998. Migrating Cretaceous–Eocene Magmatismin the Serra do Mar Alkaline Province, SE Brazil: Melts from the Deflected Trindade Mantle Plume? J. Petrol. 39 (8), 1493–1526.

Torsvik, T.H., Rousse, S., Labails, C., Smethurst, M.A., 2009. A new scheme for the opening of the South Atlantic Ocean and the dissection of an Aptian salt basin. Geophys. J. Int. 177 (3), 1315–1333.

van der Beek, P., Andriessen, P., Cloetingh, S., 1995. Morphotectonic evolution of rifted continental margins: Inferences from a coupled tectonic-surface processes model and fission track thermochronology. Tectonics 14 (2), 406–421.

Wildner, W., Lima, E.F., Nardi, L.V.S., Sommer, C.A., 2002. Volcanic cycles and setting in

the neoproterozoic III to Ordovician Camaquã Basin Succession in Southern Brazil: characteristics of post-collisional magmatism. J. Volcanol. Geotherm. Res. 118, 261–283.
Wildner, W., Ramgrab, G.E., Lopes, R.C., Iglesias, C.M.F., 2006. Mapa geologico do Estado do Rio Grande do Sul, Escala 1:750.000. CPRM, Porto Alegre.
Wildman, M., Cogné, N., Beucher, R., 2019. Fission-track thermochronology applied to the evolution of passive continental margins. In: Malusà, M.G., Fitzgerald, P.G. (Eds.), Fission-Track Thermochronology and its Application to Geology. Springer, pp. 351–371.
Will, T.M., Frimmel, H.E., 2018. Where does a continent prefer to break up? Some lessons from the South Atlantic margins. Gondwana Res. 53, 9–19.
Zalán, P.V., Wolff, S., Astolfi, M.A.M., Vieira, I.S., Conceição, J.C.J., Appi, V.T., Santos Neto, E.V., Cerqueira, J.R., Marques, A., 1990. The Paraná Basin, Brazil. In: In: Leighton, M.W., Kolata, D.R., Oltz, D.F., Eidel, J.J. (Eds.), Interior Cratonic Basins. American Association of Petroleum Geologists Memoir 51. pp. 681–708.
Zeitler, P.K., Enkelmann, E., Thomas, J.B., Watson, E.B., Ancuta, L.D., Idleman, B.D., 2017. Solubility and trapping of helium in apatite. Geochim. Cosmochim. Acta 209, 1–8.
Zerfass, H., Chemale Jr., F., Schultz, C.L., Lavina, E., 2004. Tectonics and sedimentation in Southern South America during triassic. Sediment. Geol. 166, 265–292.